

Cross: Efficient Low-rank Tensor Completion

Anru Zhang*

University of Wisconsin-Madison

November 4, 2016

Abstract

The completion of tensors, or high-order arrays, attracts significant attention in recent research. Current literature on tensor completion primarily focuses on recovery from a set of uniformly randomly measured entries, and the required number of measurements to achieve recovery is not guaranteed to be optimal. In addition, the implementation of some previous methods are NP-hard. In this article, we propose a framework for low-rank tensor completion via a novel tensor measurement scheme we name Cross. The proposed procedure is efficient and easy to implement. In particular, we show that a third order tensor of Tucker rank- (r_1, r_2, r_3) in p_1 -by- p_2 -by- p_3 dimensional space can be recovered from as few as $r_1 r_2 r_3 + r_1(p_1 - r_1) + r_2(p_2 - r_2) + r_3(p_3 - r_3)$ noiseless measurements, which matches the sample complexity lower-bound. In the case of noisy measurements, we also develop a theoretical upper bound and the matching minimax lower bound for recovery error over certain classes of low-rank tensors for the proposed procedure. The results can be further extended to fourth or higher-order tensors. Simulation studies show that the method performs well under a variety of settings. Finally, the procedure is illustrated through a real dataset in neuroimaging.

1 Introduction

Tensors, or high-order arrays, commonly arise in a wide range of applications, including neuroimaging (Zhou et al., 2013; Li et al., 2013; Guhaniyogi et al., 2015; Li and Zhang, 2016; Sun

*E-mail address: anruzhang@stat.wisc.edu

and Li, 2016), recommender systems (Karatzoglou et al., 2010; Rendle and Schmidt-Thieme, 2010; Sun et al., 2015), hyperspectral image compression (Li and Li, 2010), multi-energy computed tomography (Semerci et al., 2014; Li et al., 2014) and computer vision (Liu et al., 2013). With the development of neuroscience and information technologies, the scales of tensor data are increasing rapidly, making the storage and computation of tensors more and more costly and difficult. For example, to simultaneously analyze 100 MRI (magnetic resonance imaging) images with dimensions 256-by-256-by-256, it would require $100 \times 256^3 = 1,677,721,600$ measurements and about 6GB of storage space.

Tensor completion, whose central goal is to recover low-rank tensors based on limited numbers of measurable entries, can be used for compression and decompression of high-dimensional low-rank tensors. Such problems have been central and well-studied for order-2 tensors (i.e. matrices) in the fields of high-dimensional statistics and machine learning for the last decade. A non-exhaustive list of references include Keshavan et al. (2009); Candès and Tao (2010); Koltchinskii et al. (2011); Rohde et al. (2011); Negahban and Wainwright (2011); Agarwal et al. (2012); Cai and Zhang (2015); Cai et al. (2016); Cai and Zhou (2016). There are efficient procedures for matrix completion with strong theoretical guarantees. Particularly, for a p_1 -by- p_2 matrix of rank- r , whenever roughly $O(r(p_1 + p_2)\text{polylog}(p_1 + p_2))$ uniformly randomly selected entries are observed, one can achieve nice recovery with high probability using convex algorithms such as matrix nuclear norm minimization (Candès and Tao, 2010; Recht, 2011) and max-norm minimization (Srebro and Shraibman, 2005; Cai and Zhou, 2016). For matrix completion, the required number of measurements nearly matches the degrees of freedom, $O((p_1 + p_2)r)$, for p_1 -by- p_2 matrices of rank- r .

Although significant progress has been made for matrix completion, similar problems for order-3 or higher tensors are far more difficult. There have been some recent literature, including Gandy et al. (2011); Kressner et al. (2014); Yuan and Zhang (2014); Mu et al. (2014); Bhojanapalli and Sanghavi (2015); Shah et al. (2015); Barak and Moitra (2016); Yuan and Zhang (2016), that studied tensor completion based on similar formulations. To be specific, let $\mathbf{X} \in \mathbb{R}^{p_1 \times p_2 \times p_3}$ be an order-3 low-rank tensor, and Ω be a subset of $[1 : p_1] \times [1 : p_2] \times [1 : p_3]$. The goal of tensor completion is to recover \mathbf{X} based on the observable entries indexed by Ω . Most of the previous literature focuses on the setting where the indices of the observable entries are uniformly ran-

domly selected. For example, Gandy et al. (2011); Liu et al. (2013) proposed the matricization nuclear norm minimization, which requires $O(rp^2 \text{polylog}(p))$ observations to recover order-3 tensors of dimension p -by- p -by- p and Tucker rank- (r, r, r) . Later, Jain and Oh (2014); Bhojanapalli and Sanghavi (2015) considered an alternative minimization method for completion of low-rank tensors with CP decomposition and orthogonal factors. Yuan and Zhang (2014, 2016) proposed the tensor nuclear norm minimization algorithm for tensor completion with noiseless observations and further proved that their proposed method has guaranteed performance for p -by- p -by- p tensors of Tucker rank- (r, r, r) with high probability when $|\Omega| \geq O((r^{1/2}p^{3/2} + r^2p)\text{polylog}(p))$. However, it is unclear whether the required number of measurements in this literature could be further improved or not. In addition, most of these proposed procedures, such as tensor matrix nuclear norm minimization, are proved to be computationally NP-hard, making them very difficult to apply in real problems.

In this paper, we propose a novel tensor measurement scheme and the corresponding efficient low-rank tensor completion algorithm. We name our methods *Cross Tensor Measurement Scheme* because the measurement set is in the shape of a high-dimensional cross contained in the tensor. We show that one can recover an unknown, Tucker rank- (r_1, r_2, r_3) , and p_1 -by- p_2 -by- p_3 tensor \mathbf{X} with

$$|\Omega| = r_1 r_2 r_3 + r_1(p_1 - r_1) + r_2(p_2 - r_2) + r_3(p_3 - r_3)$$

noiseless Cross tensor measurements. This outperforms the previous methods in literature, and matches the degrees of freedom for all rank- (r_1, r_2, r_3) tensors of dimensions p_1 -by- p_2 -by- p_3 . To the best of our knowledge, we are among the first to achieve this optimal rate. We also develop the corresponding recovery method for more general cases where measurements are taken with noise. The central idea is to transform the observable matricizations by singular value decomposition and perform the adaptive trimming scheme to denoise each block.

To illustrate the properties of the proposed procedure, both theoretical analyses and simulation studies are provided. We derive upper and lower bound results to show that the proposed recovery procedure can accommodate different levels of noise and achieve the optimal rate of convergence for a large class of low-rank tensors. Although the exact low-rank assumption is used in the theoretical analysis, some simulation settings show that such an assumption is not really necessary in practice, as long as the singular values of each matricization of the original

tensor decays sufficiently.

It is worth emphasizing that because the proposed algorithms only involve basic matrix operations such as matrix multiplication and singular value decomposition, it is tuning-free in many general situations and can be implemented efficiently to handle large scale problems. In fact, our simulation study shows that the recovery of a 500-by-500-by-500 tensor can be done stably within, on average, 10 seconds.

We also apply the proposed procedure to a 3-d MRI imaging dataset that comes from a study on Attention-deficit/hyperactivity disorder (ADHD). We show that with a limited number of Cross tensor measurements and the corresponding tensor completion algorithm, one can estimate the underlying low-rank structure of 3-d images as well as if one observes all entries of the image.

This work also relates to some previous results other than tensor completion in the literature. Mahoney et al. (2008) considered the tensor CUR decomposition, which aims to represent the tensor as the product of a sub-tensor and two matrices. However, simply applying their work cannot lead to optimal results in tensor completion since treating tensors as matrix slices would lose useful structures of tensors. Krishnamurthy and Singh (2013) proposed a sequential tensor completion algorithm under adaptive samplings. Their result requires $O(pr^{2.5} \log(r))$ number of entries for p -by- p -by- p order-3 tensors under the more restrictive CP rank- r condition, which is much larger than that of our method. Rauhut et al. (2016) considered a tensor recovery setting where each observation is a general linear projections of the original tensor. However, their theoretical analysis heavily relies on a conjecture that is difficult to check.

The rest of the paper is organized as follows. After an introduction to the notations and preliminaries in Section 2.1, we present the Cross tensor measurement scheme in Section 2.2. Based on the proposed measurement scheme, the tensor completion algorithms for both noiseless and noisy case are introduced in Sections 2.3 and 2.4 respectively. We further analyze the theoretical performance of the proposed algorithms in Section 3. The numerical performance of algorithms are investigated in a variety of simulation studies in Section 4. We then apply the proposed procedure to a real dataset of brain MRI imaging in Section 5. The proofs of the main results are finally collected in Section 6 and the supplementary materials. Although the presentation of this paper focuses on order-3 tensors, our methods can be easily extended to

fourth or higher order tensors.

2 Cross Tensor Measurements & Completion: Methodology

2.1 Basic Notations and Preliminaries

We start with basic notations and results that will be used throughout the paper. The upper case letters, e.g., X, Y, Z , are generally used to represent matrices. For $X \in \mathbb{R}^{p_1 \times p_2}$, the singular value decomposition can be written as $X = U\Sigma V^\top$. Suppose $\text{diag}(\Sigma) = (\sigma_1(X), \dots, \sigma_{\min\{p_1, p_2\}}(X))$, then $\sigma_1(X) \geq \sigma_2(X) \geq \dots \geq \sigma_{\min\{p_1, p_2\}}(X) \geq 0$ are the singular values of X . Especially, we note $\sigma_{\min}(X) = \sigma_{\min\{p_1, p_2\}}(X)$ and $\sigma_{\max}(X) = \sigma_1(X)$ as the smallest and largest singular value of X . Additionally, the matrix spectral norm and Frobenius norm are denoted as $\|X\| = \max_{u \in \mathbb{R}^{p_2}} \frac{\|Xu\|_2}{\|u\|_2}$ and $\|X\|_F = \sqrt{\sum_{i=1}^{p_1} \sum_{j=1}^{p_2} X_{ij}^2} = \sqrt{\sum_{i=1}^{\min\{p_1, p_2\}} \sigma_i^2(X)}$, respectively. We denote $\mathbb{P}_X \in \mathbb{R}^{p_1 \times p_1}$ as the projection operator onto the column space of X . Specifically, $\mathbb{P}_X = X(X^\top X)^\dagger X^\top = XX^\dagger$. Here $(\cdot)^\dagger$ is the Moore-Penrose pseudo-inverse. Let $\mathbb{O}_{p,r}$ be the set of all p -by- r orthogonal columns, i.e., $\mathbb{O}_{p,r} = \{V \in \mathbb{R}^{p \times r} : VV^\top = I_r\}$, where I_r represents the identity matrix of dimension r .

We use bold upper case letters, e.g., $\mathbf{X}, \mathbf{Y}, \mathbf{Z}$ to denote tensors. If $\mathbf{X} \in \mathbb{R}^{p_1 \times p_2 \times p_3}$, $E_t \in \mathbb{R}^{m_t \times p_t}$, $t = 1, 2, 3$. The *mode products* (tensor-matrix product) is defined as

$$\mathbf{X} \times_1 E_1 \in \mathbb{R}^{m_1 \times p_2 \times p_3}, \quad (\mathbf{X} \times_1 E_1)_{ijk} = \sum_{s=1}^{p_1} E_{1, is} \mathbf{X}_{sjk}, \quad i \in [1 : m_1], j \in [1 : p_2], k \in [1 : p_3].$$

The mode-2 product $\mathbf{X} \times_2 E_2$ and mode-3 product $\mathbf{X} \times_3 E_3$ can be defined similarly. Interestingly, the products along different modes satisfy the commutative law, e.g., $\mathbf{X} \times_t E_t \times_s E_s = \mathbf{X} \times_s E_s \times_t E_t$ if $s \neq t$. The *matricization* (or unfolding, flattening in literature), $\mathcal{M}_t(\mathbf{X})$, maps a tensor $\mathbf{X} \in \mathbb{R}^{p_1 \times p_2 \times p_3}$ into a matrix $\mathcal{M}_t(\mathbf{X}) \in \mathbb{R}^{p_t \times \prod_{s \neq t} p_s}$, so that for any $i \in \{1, \dots, p_1\}, j \in \{1, \dots, p_2\}, k \in \{1, \dots, p_3\}$,

$$\mathbf{X}_{ijk} = (\mathcal{M}_1(\mathbf{X}))_{[i, (j+p_2(k-1))]} = (\mathcal{M}_2(\mathbf{X}))_{[j, (k+p_3(i-1))]} = (\mathcal{M}_3(\mathbf{X}))_{[k, (i+p_1(j-1))]}.$$

The tensor Hilbert Schmitt norm and tensor spectral norm, which are defined as

$$\|\mathbf{X}\|_{\text{HS}} = \sqrt{\sum_{i=1}^{p_1} \sum_{j=1}^{p_2} \sum_{k=1}^{p_3} \mathbf{X}_{ijk}^2}, \quad \|\mathbf{X}\|_{\text{op}} = \max_{u \in \mathbb{R}^{p_1}, v \in \mathbb{R}^{p_2}, w \in \mathbb{R}^{p_3}} \frac{\mathbf{X} \times_1 u \times_2 v \times_3 w}{\|u\|_2 \|v\|_2 \|w\|_2},$$

will be intensively used in this paper. It is also noteworthy that the general calculation of the tensor operator norm is NP-hard (Hillar and Lim, 2013). Unlike matrices, there is no universal definition of rank for third or higher order tensors. Standing out from various definitions, the *Tucker rank* (Tucker, 1966) has been widely utilized in literature, and its definition is closely associated with the following *Tucker decomposition*: for $\mathbf{X} \in \mathbb{R}^{p_1 \times p_2 \times p_3}$,

$$\mathbf{X} = \mathbf{S} \times_1 U_1 \times_2 U_2 \times_3 U_3, \quad \text{or equivalently} \quad \mathbf{X}_{ijk} = \sum_{i'j'k'} s_{i'j'k'} U_{1,ii'} U_{2,jj'} U_{3,kk'}. \quad (1)$$

Here $\mathbf{S} \in \mathbb{R}^{r_1 \times r_2 \times r_3}$ is referred to as the *core tensor*, $U_k \in \mathbb{O}_{p_k, r_k}$. The minimum number of triplets (r_1, r_2, r_3) are defined as the *Tucker rank* of \mathbf{X} which we denote as $\text{rank}(\mathbf{X}) = (r_1, r_2, r_3)$. The Tucker rank can be calculated easily by the rank of each matricization: $r_t = \text{rank}(\mathcal{M}_t(\mathbf{X}))$. It is also easy to prove that the triplet (r_1, r_2, r_3) satisfies $r_t \leq p_t$, $\max^2\{r_1, r_2, r_3\} \leq r_1 r_2 r_3$. For a more detailed survey of tensor decomposition, readers are referred to Kolda and Bader (2009).

We also use the following symbols to represent sub-arrays. For any subsets Ω_1, Ω_2 , etc, we use $X_{[\Omega_1, \Omega_2]}$ to represent the sub-matrix of X with row indices Ω_1 and column indices Ω_2 . The sub-tensors are denoted similarly: $\mathbf{X}_{[\Omega_1, \Omega_2, \Omega_3]}$ represents the tensors with mode- t indices in Ω_t for $t = 1, 2, 3$. For better presentation, we use bracket to represent index sets. Particularly for any integers $a \leq b$, let $[a : b] = \{a, \dots, b\}$ and let “:” alone represent the whole index set. Thus, $U_{[:, 1:r]}$ represents the first r columns of U ; $\mathbf{X}_{[\Omega_1, \Omega_2, :]}$ represents the sub-tensor of \mathbf{X} with mode-1 indices Ω_1 , mode-2 indices Ω_2 and all mode-3 indices.

Now we establish the lower bound for the minimum number of measurements for Tucker low-rank tensor completion based on counting the degrees of freedom.

Proposition 1 (Degrees of freedom for rank- (r_1, r_2, r_3) tensors in $\mathbb{R}^{p_1 \times p_2 \times p_3}$) Assume that $r_1 \leq p_1, r_2 \leq p_2, r_3 \leq p_3$, $\max^2\{r_1, r_2, r_3\} \leq r_1 r_2 r_3$, then the degrees of freedom of all rank- (r_1, r_2, r_3) tensors in $\mathbb{R}^{p_1 \times p_2 \times p_3}$ is

$$r_1 r_2 r_3 + (p_1 - r_1) r_1 + (p_2 - r_2) r_2 + (p_3 - r_3) r_3.$$

Remark 1 Beyond order-3 tensors, we can show the degrees of freedom for rank- (r_1, \dots, r_d) order- d tensors in $\mathbb{R}^{p_1 \times \dots \times p_d}$ is $\prod_{t=1}^d r_t + \sum_{t=1}^d r_t (p_t - r_t)$ similarly.

Proposition 1 provides a lower bound and the benchmark for the number of measurements to guarantee low-rank tensor completion, i.e., $r_1 r_2 r_3 + \sum_{t=1}^3 r_t(p_t - r_t)$. Since the previous methods are not guaranteed to achieve this lower bound, we focus on developing the first measurement scheme that can both work efficiently and reach this benchmark.

2.2 Cross Tensor Measurements

In this section, we propose a novel Cross tensor measurement scheme. Suppose the targeting unknown tensor \mathbf{X} is of p_1 -by- p_2 -by- p_3 , we let

$$\begin{aligned} \Omega_1 &\subseteq [1 : p_1], \quad \Omega_2 \subseteq [1 : p_2], \quad \Omega_3 \subseteq [1 : p_3], \quad \text{where} \quad |\Omega_t| = m_t, \quad t = 1, 2, 3; \\ \Xi_1 &\subseteq \Omega_2 \times \Omega_3, \quad \Xi_2 \subseteq \Omega_3 \times \Omega_1, \quad \Xi_3 \subseteq \Omega_1 \times \Omega_2, \quad \text{where} \quad |\Xi_t| = g_t, \quad t = 1, 2, 3. \end{aligned} \quad (2)$$

Then we measure the entries of \mathbf{X} using the following indices set

$$\mathbf{\Omega} = (\Omega_1 \times \Omega_2 \times \Omega_3) \cup ([1 : p_1] \times \Xi_1) \cup ([1 : p_2] \times \Xi_2) \cup ([1 : p_3] \times \Xi_3) \subseteq [1 : p_1, 1 : p_2, 1 : p_3], \quad (3)$$

where

$$\begin{aligned} \Omega_1 \times \Omega_2 \times \Omega_3 &= \{(i, j, k) : i \in \Omega_1, j \in \Omega_2, k \in \Omega_3\} \quad \text{are referred to as } \textit{body measurements}; \\ \left. \begin{aligned} [1 : p_1] \times \Xi_1 &= \{(i, j, k) : i \in [1 : p_1], (j, k) \in \Xi_1\} \\ [1 : p_2] \times \Xi_2 &= \{(i, j, k) : j \in [1 : p_2], (k, i) \in \Xi_2\} \\ [1 : p_3] \times \Xi_3 &= \{(i, j, k) : k \in [1 : p_3], (i, j) \in \Xi_3\} \end{aligned} \right\} \quad \text{are referred to as } \textit{arm measurements}. \end{aligned} \quad (4)$$

Meanwhile, the intersections among body and arm measurements, which we refer to as *joint measurements*, also play important roles in our analysis:

$$\begin{aligned} \Omega_1 \times \Xi_1 &= (\Omega_1 \times \Omega_2 \times \Omega_3) \cap ([1 : p_1] \times \Xi_1) = \{(i, j, k) : i \in \Omega_1, (j, k) \in \Xi_1\}, \\ \Omega_2 \times \Xi_2 &= (\Omega_1 \times \Omega_2 \times \Omega_3) \cap ([1 : p_2] \times \Xi_2) = \{(i, j, k) : j \in \Omega_2, (k, i) \in \Xi_2\}, \\ \Omega_3 \times \Xi_3 &= (\Omega_1 \times \Omega_2 \times \Omega_3) \cap ([1 : p_3] \times \Xi_3) = \{(i, j, k) : k \in \Omega_3, (i, j) \in \Xi_3\}. \end{aligned} \quad (5)$$

A pictorial illustration of the body, arm and joint measurements is provided in Figure 1. Since the measurements are generally cross-shaped, we refer to $\mathbf{\Omega}$ as the *Cross Tensor Measurement Scheme*. It is easy to see that the total number of measurements for the proposed scheme is $m_1 m_2 m_3 + g_1(p_1 - m_1) + g_2(p_2 - m_2) + g_3(p_3 - m_3)$ and the sampling ratio is

$$\frac{\# \text{Observable samples}}{\# \text{All parameters}} = \frac{m_1 m_2 m_3 + g_1(p_1 - m_1) + g_2(p_2 - m_2) + g_3(p_3 - m_3)}{p_1 p_2 p_3}. \quad (6)$$

Based on these measurements, we focus on the following model,

$$\mathbf{Y}_\Omega = \mathbf{X}_\Omega + \mathbf{Z}_\Omega, \quad \text{i.e.} \quad Y_{ijk} = X_{ijk} + Z_{ijk}, \quad (i, j, k) \in \Omega, \quad (7)$$

where \mathbf{X} , \mathbf{Y} and \mathbf{Z} correspond to the original tensor, observed values and unknown noise term, respectively.

2.3 Recovery Algorithm – Noiseless Case

When \mathbf{X} is exactly low-rank and the observations are noiseless, i.e. $\mathbf{Y}_{ijk} = \mathbf{X}_{ijk}$, we can recover \mathbf{X} with the following algorithm. We first construct the *arm matricizations*, *joint matricizations* and *body matricizations* based on (4) and (5),

$$Y_{\Xi_t} = \mathcal{M}_t(\mathbf{Y}_{[1:p_t] \times \Xi_t}) \in \mathbb{R}^{p_t \times g_t}, \quad (\text{Arm matricizations}) \quad (8)$$

$$Y_{t,\Omega} = \mathcal{M}_t(\mathbf{Y}_{[\Omega_1, \Omega_2, \Omega_3]}) \in \mathbb{R}^{m_t \times \prod_{s \neq t} m_s}, \quad (\text{Body matricizations}) \quad (9)$$

$$Y_{\Omega_t \times \Xi_t} = \mathcal{M}_t(\mathbf{Y}_{\Omega_t \times \Xi_t}) \in \mathbb{R}^{m_t \times g_t}. \quad (\text{Joint matricizations}) \quad (10)$$

In the noiseless setting, we propose the following formula to complete \mathbf{X} :

$$\hat{\mathbf{X}} = \mathbf{Y}_{[\Omega_1, \Omega_2, \Omega_3]} \times_1 R_1 \times_2 R_2 \times_3 R_3, \quad (11)$$

$$R_1 = Y_{\Xi_1} Y_{\Omega_1 \times \Xi_1}^\dagger \in \mathbb{R}^{p_1 \times m_1}, \quad R_2 = Y_{\Xi_2} Y_{\Omega_2 \times \Xi_2}^\dagger \in \mathbb{R}^{p_2 \times m_2}, \quad R_3 = Y_{\Xi_3} Y_{\Omega_3 \times \Xi_3}^\dagger \in \mathbb{R}^{p_3 \times m_3}. \quad (12)$$

The procedure is summarized in Algorithm 1. The theoretical guarantee for this proposed algorithm is provided in Theorem 1.

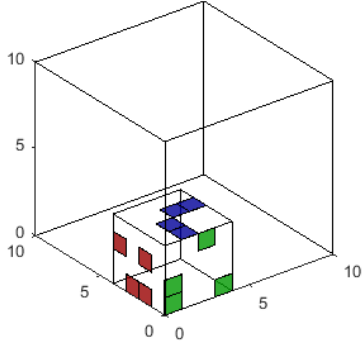
Algorithm 1 Cross: Efficient Algorithm for Tensor Completion with Noiseless Observations

- 1: Input: noiseless observations \mathbf{Y}_{ijk} , $(i, j, k) \in \Omega$ from (3).
- 2: Construct $Y_{\Xi_1}, Y_{\Xi_2}, Y_{\Xi_3}, Y_{\Omega_1 \times \Xi_1}, Y_{\Omega_2 \times \Xi_2}, Y_{\Omega_3 \times \Xi_3}$ as (8).
- 3: Calculate

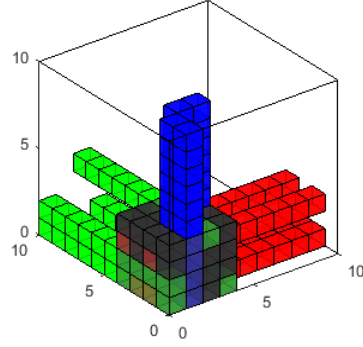
$$R_1 = Y_{\Xi_1} Y_{\Omega_1 \times \Xi_1}^\dagger \in \mathbb{R}^{p_1 \times m_1}, \quad R_2 = Y_{\Xi_2} Y_{\Omega_2 \times \Xi_2}^\dagger \in \mathbb{R}^{p_2 \times m_2}, \quad R_3 = Y_{\Xi_3} Y_{\Omega_3 \times \Xi_3}^\dagger \in \mathbb{R}^{p_3 \times m_3}.$$

- 4: Calculate the final estimator

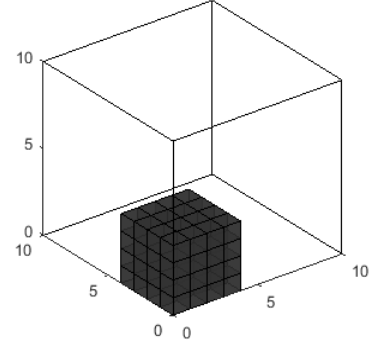
$$\hat{\mathbf{X}} = \mathbf{Y}_{[\Omega_1, \Omega_2, \Omega_3]} \times_1 R_1 \times_2 R_2 \times_3 R_3.$$



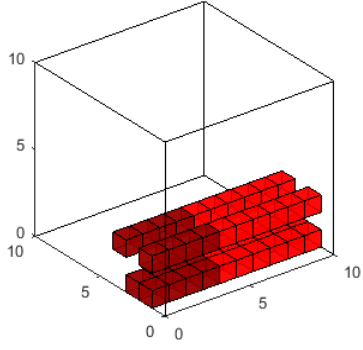
(a) Ω_t, Ξ_t illustration



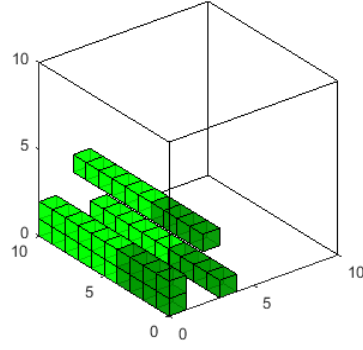
(b) All measurements



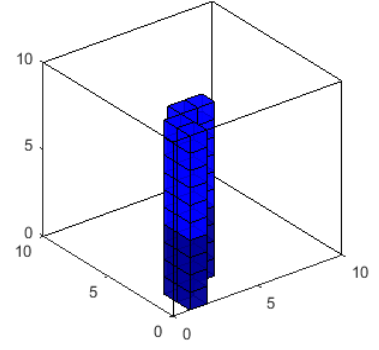
(c) Body measurements $\mathbf{Y}_{[\Omega_1, \Omega_2, \Omega_3]}$



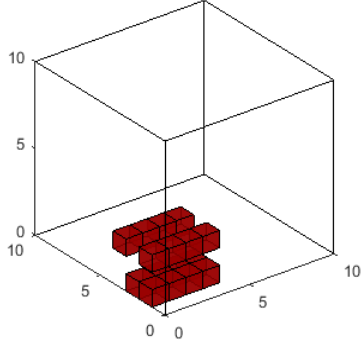
(d) Arm measurements \mathbf{Y}_{Ξ_1}



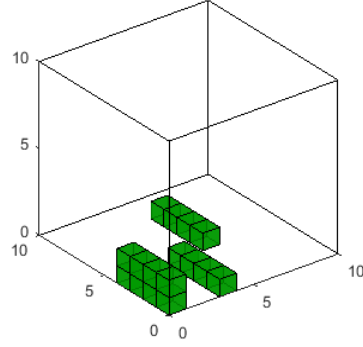
(e) Arm measurements \mathbf{Y}_{Ξ_2}



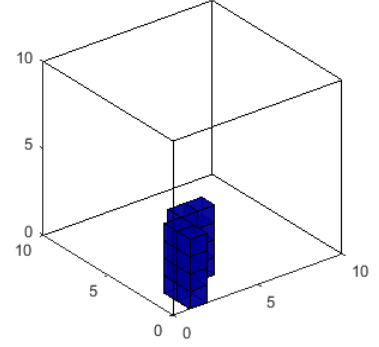
(f) Arm measurements \mathbf{Y}_{Ξ_3}



(g) Joint measurements $\mathbf{Y}_{\Omega_1 \times \Xi_1}$



(h) Joint measurements $\mathbf{Y}_{\Omega_2 \times \Xi_2}$



(i) Joint measurements $\mathbf{Y}_{\Omega_3 \times \Xi_3}$

Figure 1: Illustrative example for Cross Tensor Measurements Scheme. For better illustration here we assume $\Omega_t = [1 : m_t]$, $p_1 = p_2 = p_3 = 10$, $m_1 = m_2 = m_3 = g_1 = g_2 = g_3 = 4$.

Theorem 1 (Exact recovery in noiseless setting) Suppose $\mathbf{X} \in \mathbb{R}^{p_1 \times p_2 \times p_3}$, $\text{rank}(\mathbf{X}) = (r_1, r_2, r_3)$. Assume all Cross tensor measurements are noiseless, i.e. $\mathbf{Y}_\Omega = \mathbf{X}_\Omega$. If $r_t \leq \min\{m_t, g_t\}$ and $\text{rank}(Y_{\Omega_t \times \Xi_t}) = r_t$ for $t = 1, 2, 3$, then

$$\mathbf{X} = \mathbf{Y}_{[\Omega_1, \Omega_2, \Omega_3]} \times_1 R_1 \times_2 R_2 \times_3 R_3, \quad \text{where} \quad R_t = Y_{\Xi_t} Y_{\Omega_t \times \Xi_t}^\dagger, \quad t = 1, 2, 3. \quad (13)$$

Moreover, if there are $\tilde{M}_t \in \mathbb{R}^{m_t \times r_t}$, $\tilde{N}_t \in \mathbb{R}^{g_t \times r_t}$ such that $\tilde{M}_t^\top X_{\Omega_t \times \Xi_t} \tilde{N}_t \in \mathbb{R}^{r_t \times r_t}$ is non-singular for $t = 1, 2, 3$, then we further have

$$\mathbf{X} = \mathbf{Y}_{[\Omega_1, \Omega_2, \Omega_3]} \times_1 \tilde{R}_1 \times_2 \tilde{R}_2 \times_3 \tilde{R}_3, \quad \text{where} \quad \tilde{R}_t = Y_{\Xi_t} \tilde{N}_t^\top \left(\tilde{M}_t^\top Y_{\Omega_t \times \Xi_t} \tilde{N}_t \right)^{-1} \tilde{M}_t^\top, \quad t = 1, 2, 3. \quad (14)$$

Theorem 1 shows that, in the noiseless setting, as long as $r_t \leq \min\{m_t, g_t\}$ and the joint matricizations $Y_{\Omega_t \times \Xi_t}$ have the same rank as $\mathcal{M}_t(\mathbf{X})$, exact recovery by Algorithm 1 can be guaranteed. Therefore when $m_t = g_t = r_t$, the minimum required number of measurements for the proposed Cross tensor measurement scheme is $r_1 r_2 r_3 + r_1(p_1 - r_1) + r_2(p_2 - r_2) + r_3(p_3 - r_3)$ when we set $m_t = g_t = r_t$, which exactly matches the lower bound established in Proposition 1 and outperforms the previous methods in the literature.

On the other hand, Algorithm 1 heavily relies on the noiseless assumption. In fact, calculating $Y_{\Omega_t \times \Xi_t}^\dagger = (X_{\Omega_t \times \Xi_t} + Z_{\Omega_t \times \Xi_t})^\dagger$ is unstable even with low levels of noise, which ruins the performance of Algorithm 1. Since we rarely have noiseless observations in practice, we focus on the setting with non-zero noise for the rest of the paper.

2.4 Recovery Algorithm – Noisy Case

In this section we propose the following procedure for recovery in the noisy setting. The proposed algorithm is divided into four steps and an illustrative example is provided in Figure 2 for readers' better understanding.

- **(Step 1: Construction of Matricizations)** Same as Algorithm 1, Construct the *arm*, *body* and *joint matricizations* as (8) and (9) (see Figure 2(a)),

$$\text{Arm: } Y_{\Xi_1}, Y_{\Xi_2}, Y_{\Xi_3}, \quad \text{Body: } Y_{1, \Omega}, Y_{2, \Omega}, Y_{3, \Omega}, \quad \text{Joint: } Y_{\Omega_1 \times \Xi_1}, Y_{\Omega_2 \times \Xi_2}, Y_{\Omega_3 \times \Xi_3}.$$

- **(Step 2: Rotation)** For $t = 1, 2, 3$, we calculate the singular value decompositions of Y_{Ξ_t} and $Y_{t,\Omega}$, then store

$$\begin{aligned} V_t^{(A)} &\in \mathbb{O}_{g_t} \quad \text{as the right singular vectors of } Y_{\Xi_t}, \\ U_t^{(B)} &\in \mathbb{O}_{m_t} \quad \text{as the left singular vectors of } Y_{t,\Omega}. \end{aligned} \quad (15)$$

Here the superscripts “(A), (B)” represent arm and body, respectively. We calculate the following rotation for arm and joint matricizations based on SVDs (See Figure 2(b), (c)).

$$\begin{aligned} A_t &= Y_{\Xi_t} \cdot V_t^{(A)} \in \mathbb{R}^{p_t \times g_t}, \\ J_t &= (U_t^{(B)})^\top \cdot Y_{\Omega_t \times \Xi_t} \cdot V_t^{(A)} \in \mathbb{R}^{m_t \times g_t}. \end{aligned} \quad (16)$$

As we can see from Figure 2(c), the magnitude of A_t ’s columns and J_t ’s both columns and rows decreases front to back. Therefore, the important factors of Y_{Ξ_t} and $Y_{\Omega_t \times \Xi_t}$ are moved to front rows and columns in this step.

- **(Step 3: Adaptive Trimming)** Since A_t and J_t are contaminated with noise, in this step we denoise them by trimming the lower ranking columns of A_t and both lower ranking columns and rows of J_t . To decide the number of rows and columns to trim, it will be good to have an estimate for (r_1, r_2, r_3) , say $(\hat{r}_1, \hat{r}_2, \hat{r}_3)$. We will show later in theoretical analysis that a good choice of \hat{r}_t should satisfy

$$(J_t)_{[1:\hat{r}_t, 1:\hat{r}_t]} \text{ is non-singular} \quad \text{and} \quad \left\| (A_t)_{[:, 1:\hat{r}_t]} (J_t)_{[1:\hat{r}_t, 1:\hat{r}_t]}^{-1} \right\| \leq \lambda_t, \quad t = 1, 2, 3. \quad (17)$$

λ_t is the tuning parameter here, and in a variety of situations we can simply choose $\lambda_t = 3\sqrt{p_t/m_t}$ for reasons we will discuss later. Our final estimator for r_t is the largest \hat{r}_t that satisfies Condition (17), and can be found by verifying (17) for all possible r_t ’s. It is worth mentioning that this step shares similar ideas with structured matrix completion in Cai et al. (2016). (See Figure 2(d) and (e)).

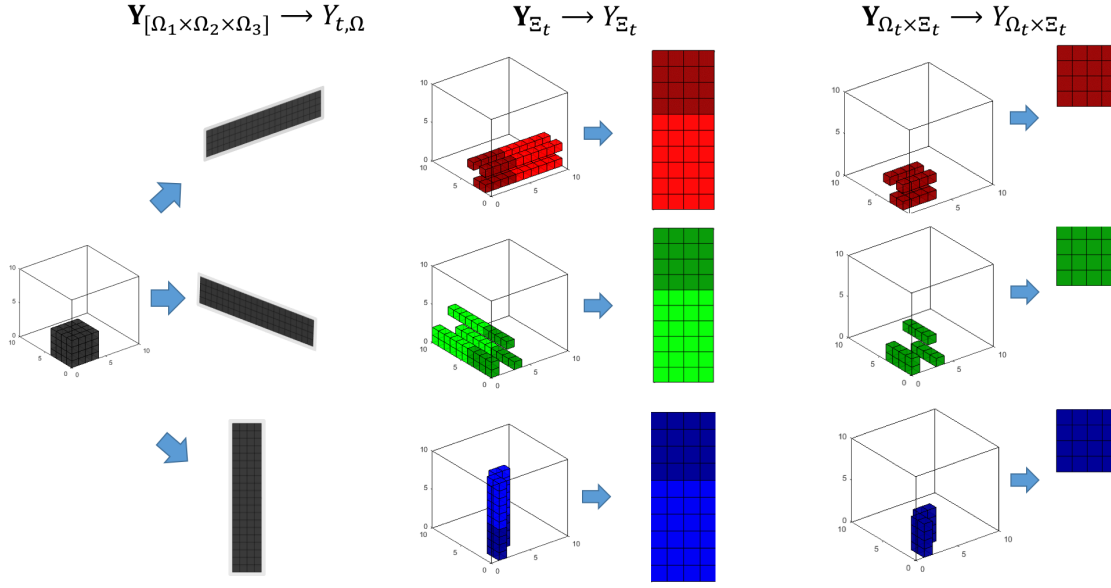
- **(Step 4: Assembling)** Finally, given $\hat{r}_1, \hat{r}_2, \hat{r}_3$ obtained from Step 3, we calculate

$$\bar{R}_t = (A_t)_{[:, 1:\hat{r}_t]} (J_t)_{[1:\hat{r}_t, 1:\hat{r}_t]}^{-1} (V_{t, [1:\hat{r}_t, :]}^{(A)})^\top \in \mathbb{R}^{p_t \times m_t}, \quad t = 1, 2, 3, \quad (18)$$

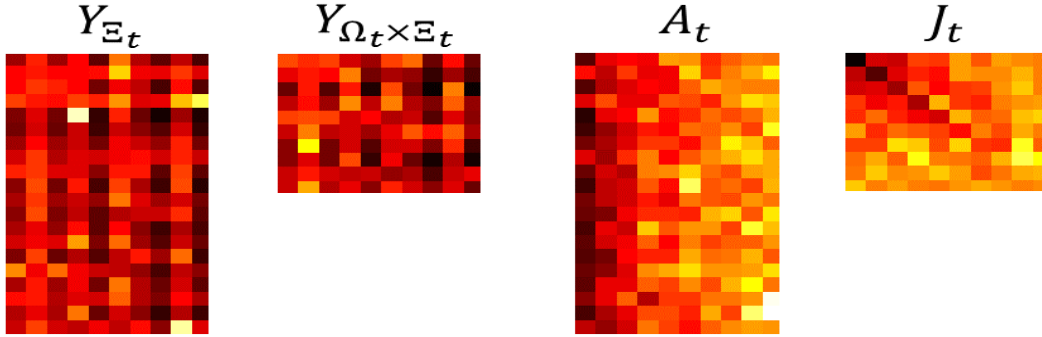
and recover the original low-rank tensor \mathbf{X} by

$$\hat{\mathbf{X}} = \mathbf{Y}_{[\Omega_1, \Omega_2, \Omega_3]} \times_1 \bar{R}_1 \times_2 \bar{R}_2 \times_3 \bar{R}_3. \quad (19)$$

The procedure is summarized as Algorithm 2. It is worth mentioning that both Algorithms 1 and 2 can be easily extended to fourth and higher order tensors.

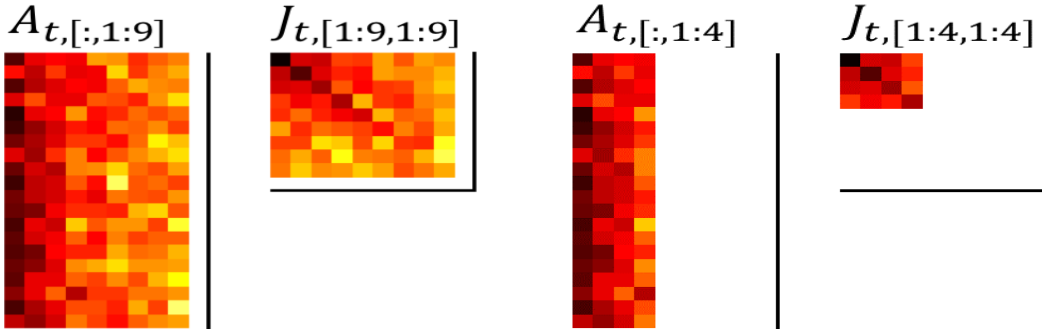


(a) Step 1. All matricizations: $Y_{t,\Omega}$, Y_{Ξ_t} and $Y_{\Omega_t \times \Xi_t}$



(b) Heatmap illustration of Y_{Ξ_t} , $Y_{\Omega_t \times \Xi_t}$ (darker blocks mean larger absolute values)

(c) Step 2. We obtain A_t , J_t after rotation



(d) Step 3. Intermediate process of trimming

(e) Step 3. Eventually located at $\hat{r}_t = 4$

Figure 2: Illustration of the proposed procedure in noisy setting

Algorithm 2 Noisy Tensor Completion with Cross Measurements

1: Input: entries \mathbf{Y}_{ijk} , $(i, j, k) \in \Omega$ from (3), $\lambda_1, \lambda_2, \lambda_3$.

2: Construct arm, body and joint matricizations as (8) and (9),

$$Y_{\Xi_t} \in \mathbb{R}^{p_t \times g_t}, \quad Y_{\Omega_t \times \Xi_t} \in \mathbb{R}^{m_t \times g_t}, \quad Y_{t, \Omega} \in \mathbb{R}^{m_t \times (\prod_{s \neq t} m_s)}, \quad t = 1, 2, 3.$$

3: Calculate $U_t^{(B)}$ and $V_t^{(A)}$ via SVDs:

$$U_t^{(B)} \in \mathbb{O}_{m_t}, \text{ as the left singular vectors of } X_{\Xi_t};$$

$$V_t^{(A)} \in \mathbb{O}_{g_t}, \text{ as the right singular vectors of } X_{t, \Omega}.$$

4: Rotate the arm and joint measurements as

$$A_t = X_{\Xi_t} \cdot V^{(A)} \in \mathbb{R}^{p_t \times g_t}, \quad J_t = \left(U^{(B)} \right)^\top \cdot X_{\Omega_t \times \Xi_t} \cdot V^{(A)} \in \mathbb{R}^{m_t \times g_t}.$$

5: **for** $t = 1, 2, 3$ **do**

6: **for** $s = \min\{g_t, m_t\} : -1 : 1$ **do**

7: **if** $J_{t, [1:s, 1:s]}$ is not singular and $\|A_{t, [:, 1:s]} J_{t, [1:s, 1:s]}^{-1}\| \leq \lambda_t$ **then**

8: $\hat{r}_t = s$; **break** from the loop;

9: **end if**

10: **end for**

11: **If** \hat{r}_t is still unassigned **then** $\hat{r}_t = 0$.

12: **end for**

13: Calculate

$$\bar{R}_t = A_{t, [:, 1:s]} J_{t, [1:s, 1:s]}^{-1} (V_{t, [1:\hat{r}_t, :]}^{(A)})^\top \in \mathbb{R}^{p_t \times m_t}, \quad t = 1, 2, 3.$$

14: Compute the final estimator

$$\hat{\mathbf{X}} = \mathbf{Y}_{[\Omega_1, \Omega_2, \Omega_3]} \times_1 \bar{R}_1 \times_2 \bar{R}_2 \times_3 \bar{R}_3.$$

3 Theoretical Analysis

In this section, we investigate the theoretical performance for the proposed procedure in the last section. Recall that our goal is to recover \mathbf{X} from \mathbf{Y}_Ω based on (3). Similarly, one can further define the arm, joint and body matricizations for \mathbf{X} , \mathbf{Z} , i.e. X_{Ξ_t} , $X_{\Omega_t \times \Xi_t}$, $X_{t,\Omega}$, Z_{Ξ_t} , $Z_{\Omega_t \times \Xi_t}$ and $Z_{t,\Omega}$ for $t = 1, 2, 3$ in the same fashion as Y_{Ξ_t} , $Y_{\Omega_t \times \Xi_t}$ and $Y_{t,\Omega}$ in (8), (9) and (10). We first present the following theoretical guarantees for low-rank tensor completion based on noisy observations via Algorithm 2.

Theorem 2 *Suppose $\mathbf{X} \in \mathbb{R}^{p_1 \times p_2 \times p_3}$, $\text{rank}(\mathbf{X}) = (r_1, r_2, r_3)$. Assume we observe \mathbf{Y}_Ω based on Cross tensor measurement scheme (4), where \mathbf{X}_Ω satisfies $\text{rank}(X_{\Omega_t \times \Xi_t}) = r_t$ and*

$$\sigma_{r_t}(X_{\Omega_t \times \Xi_t}) > 5 \|Z_{\Omega_t \times \Xi_t}\|, \quad \sigma_{r_t}(X_{\Xi_t}) > 5 \|Z_{\Xi_t}\|, \quad \sigma_{r_t}(X_{t,\Omega}) > 5 \|Z_{t,\Omega}\|. \quad (20)$$

We further define

$$\xi_t = \left\| X_{\Omega_t \times \Xi_t}^\dagger X_{t,\Omega} \right\|, \quad t = 1, 2, 3. \quad (21)$$

Applying Algorithm 2 with $\lambda_1, \lambda_2, \lambda_3$ satisfying

$$\lambda_t \geq 2 \left\| X_{t,\Xi_t} X_{\Omega_t \times \Xi_t}^\dagger \right\|, \quad t = 1, 2, 3, \quad (22)$$

we have the following upper bound results for some uniform constant C ,

$$\begin{aligned} \left\| \hat{\mathbf{X}} - \mathbf{X} \right\|_{\text{HS}} &\leq C \lambda_1 \lambda_2 \lambda_3 \left\| \mathbf{Z}_{[\Omega_1, \Omega_2, \Omega_3]} \right\|_{\text{HS}} + C \lambda_1 \lambda_2 \lambda_3 \left(\sum_{t=1}^3 \xi_t \|Z_{\Omega_t \times \Xi_t}\|_F + C \sum_{t=1}^3 \frac{\xi_t}{\lambda_t} \|Z_{\Xi_t}\|_F \right), \\ \left\| \hat{\mathbf{X}} - \mathbf{X} \right\|_{\text{op}} &\leq C \lambda_1 \lambda_2 \lambda_3 \left\| \mathbf{Z}_{[\Omega_1, \Omega_2, \Omega_3]} \right\|_{\text{op}} + C \lambda_1 \lambda_2 \lambda_3 \left(\sum_{t=1}^3 \xi_t \|Z_{\Omega_t \times \Xi_t}\| + C \sum_{t=1}^3 \frac{\xi_t}{\lambda_t} \|Z_{\Xi_t}\| \right). \end{aligned}$$

It is helpful to explain the meanings of the conditions used in Theorem 2. The singular value gap condition (20) is assumed in order to guarantee that signal dominates the noise in the observed blocks. λ_t and ξ_t are important factors in our analysis which represent “arm-joint” and “joint-body” ratio respectively. These factors roughly indicate how much information is contained in the body and arm measurements and how much impact the noisy terms have on the upper bound, all of which implicitly indicate the difficulty of the problem. Based on λ_t, ξ_t ,

we consider the following classes of tuples formed by rank- (r_1, r_2, r_3) tensors, the perturbation \mathbf{Z} , and indices of observations,

$$\mathcal{F} = \mathcal{F}_{\{\lambda_t\}, \{\xi_t\}} = \left\{ \begin{array}{l} \mathbf{X} \in \mathbb{R}^{p_1 \times p_2 \times p_3}, \text{rank}(\mathbf{X}) = (r_1, r_2, r_3); \\ (\mathbf{X}, \mathbf{Z}, \Omega_t, \Xi_t) : \sigma_{r_t}(X_{\Omega_t \times \Xi_t}) \geq 5\|Z_{\Omega_t \times \Xi_t}\|, \sigma_{r_t}(X_{\Xi_t}) \geq 5\|Z_{\Xi_t}\|, \sigma_{r_t}(X_{t, \Omega}) \geq 5\|Z_{t, \Omega}\|; \\ \|X_{\Xi_t} X_{\Omega_t \times \Xi_t}^\dagger\| \leq \lambda_t, \|X_{\Omega_t \times \Xi_t}^\dagger X_{t, \Omega}\| \leq \xi_t. \end{array} \right\} \quad (23)$$

and provide the following lower bound result over $\mathcal{F}_{\{\lambda_t\}, \{\xi_t\}}$.

Theorem 3 (Lower Bound) *Suppose positive integers r_t, p_t satisfy $6 \max\{r_1, r_2, r_3\}^2 \leq r_1 r_2 r_3$, $p_t \geq 2r_t$. The arm, body and joint measurement errors are bounded as*

$$\|\mathbf{Z}_{[\Omega_1, \Omega_2, \Omega_3]}\|_{\text{HS}} \leq C^{(B)}, \quad \|Z_{t, \Xi_t}\|_F \leq C_t^{(A)}, \quad \|Z_{t, \Omega_t \times \Xi_t}\|_F \leq C_t^{(J)}. \quad (24)$$

If $C_t^{(J)} \leq \min\{C_t^{(J)}, C^{(B)}\}$, $\xi_t \geq 28$, $\lambda_t > 1$, then there exists uniform constant $c > 0$ such that

$$\inf_{\hat{\mathbf{X}}} \sup_{\substack{(\mathbf{X}, \mathbf{Z}, \Omega_t, \Xi_t) \in \mathcal{F} \\ \mathbf{Z} \text{ satisfies (24)}}} \|\hat{\mathbf{X}} - \mathbf{X}\|_{\text{HS}} \geq c\lambda_1 \lambda_2 \lambda_3 C^{(B)} + c\lambda_1 \lambda_2 \lambda_3 \sum_{t=1}^3 \left(\xi_t C_t^{(J)} + \frac{\xi_t}{\lambda_t} C_t^{(A)} \right). \quad (25)$$

Similarly, suppose $C^{(B)}, C_t^{(A)}, C_t^{(J)}$ are the upper bound for arm, body and joint measurement errors in tensor and matrix operator norms respectively, i.e.

$$\|\mathbf{Z}_{[\Omega_1, \Omega_2, \Omega_3]}\|_{\text{op}} \leq C^{(B)}, \quad \|Z_{t, \Xi_t}\| \leq C_t^{(A)}, \quad \|Z_{t, \Omega_t \times \Xi_t}\| \leq C_t^{(J)}. \quad (26)$$

Suppose $C_t^{(J)} \leq \min\{C_t^{(A)}, C^{(B)}\}$, $\xi_t \geq 28$, $\lambda_t > 1$, then

$$\inf_{\hat{\mathbf{X}}} \sup_{\substack{(\mathbf{X}, \mathbf{Z}, \Omega_t, \Xi_t) \in \mathcal{F} \\ \mathbf{Z} \text{ satisfies (26)}}} \|\hat{\mathbf{X}} - \mathbf{X}\|_{\text{op}} \geq c\lambda_1 \lambda_2 \lambda_3 C^{(B)} + c\lambda_1 \lambda_2 \lambda_3 \sum_{t=1}^3 \left(\xi_t C_t^{(J)} + \frac{\xi_t}{\lambda_t} C_t^{(A)} \right). \quad (27)$$

Remark 2 *Theorems 2 and 3 together yield the optimal rate of recovery in \mathcal{F} in both Hilbert-Schmitt and operator norms:*

$$\begin{aligned} \inf_{\hat{\mathbf{X}}} \sup_{\substack{(\mathbf{X}, \mathbf{Z}, \Omega_t, \Xi_t) \in \mathcal{F} \\ \mathbf{Z} \text{ satisfies (24)}}} \|\hat{\mathbf{X}} - \mathbf{X}\|_{\text{HS}} &\asymp \lambda_1 \lambda_2 \lambda_3 \left\{ C^{(B)} + \sum_{t=1}^3 \left(\xi_t C_t^{(J)} + \frac{\xi_t}{\lambda_t} C_t^{(A)} \right) \right\}. \\ \inf_{\hat{\mathbf{X}}} \sup_{\substack{(\mathbf{X}, \mathbf{Z}, \Omega_t, \Xi_t) \in \mathcal{F} \\ \mathbf{Z} \text{ satisfies (26)}}} \|\hat{\mathbf{X}} - \mathbf{X}\|_{\text{op}} &\asymp \lambda_1 \lambda_2 \lambda_3 \left\{ C^{(B)} + \sum_{t=1}^3 \left(\xi_t C_t^{(J)} + \frac{\xi_t}{\lambda_t} C_t^{(A)} \right) \right\}. \end{aligned}$$

As we can see from the theoretical analyses, the choice of λ_t is crucial towards the recovery performance of Algorithm 2. Theorem 2 provides a guideline for such a choice depending on the unknown parameter $\|X_{\Xi_t} X_{\Omega_t \times \Xi_t}^\dagger\|$, which is hard to obtain in practice. However, we can choose $\lambda_t = 3\sqrt{p_t/m_t}$ in a variety of settings. Specifically in the analysis below, we show under random sampling scheme that $\Omega_1, \Omega_2, \Omega_3, \Xi_1, \Xi_2, \Xi_3$ are uniformly randomly selected from $[1 : p_1], [1 : p_2], [1 : p_3], \Omega_2 \times \Omega_3, \Omega_3 \times \Omega_1, \Omega_1 \times \Omega_2$, Algorithm 2 with $\lambda_t = 3\sqrt{p_t/m_t}$ will have guaranteed performance. The choice of $\lambda_t = 3\sqrt{p_t/m_t}$ will be further examined in simulation studies later.

Theorem 4 Suppose \mathbf{X} is with Tucker decomposition $\mathbf{X} = \mathbf{S} \times_1 U_1 \times_2 U_2 \times_3 U_3$, where $\mathbf{S} \in \mathbb{R}^{r_1 \times r_2 \times r_3}, U_1 \in \mathbb{O}_{p_1, r_1}, U_2 \in \mathbb{O}_{p_2, r_2}, U_3 \in \mathbb{O}_{p_3, r_3}$ and $U_1, U_2, U_3, \mathcal{M}_1(\mathbf{S} \times_2 U_2 \times_3 U_3), \mathcal{M}_2(\mathbf{S} \times_1 U_1 \times_3 U_3), \mathcal{M}_3(\mathbf{S} \times_1 U_1 \times_2 U_2)$ all satisfy the matrix incoherence conditions:

$$\frac{p_t}{r_t} \max_{1 \leq j \leq p_t} \left\| \mathbb{P}_{U_t} e_j^{(p_t)} \right\|_2^2 \leq \rho, \quad \frac{\prod_{s \neq t} p_s}{r_t} \max_{1 \leq j \leq \prod_{s \neq t} p_s} \left\| \mathbb{P}_{\mathcal{M}_t(\mathbf{S} \times_{(t+1)} U_{t+1} \times_{(t+2)} U_{t+2})^\top} \cdot e_j^{(\prod_{s \neq t} p_s)} \right\|_2^2 \leq \rho, \quad (28)$$

where $e_j^{(p)}$ is the j -th canonical basis in \mathbb{R}^p . Suppose we are given random Cross tensor measurements that Ω_t and Ξ_t are uniformly randomly chosen m_t and g_t values from $\{1, \dots, p_t\}$ and $\prod_{s \neq t} \Omega_s$, respectively. If for $t = 1, 2, 3$,

$$\sigma_{\min}(\mathcal{M}_t(\mathbf{S})) \geq \max \left\{ 10 \sqrt{\frac{p_1 p_2 p_3}{m_t g_t}} \|Z_{\Omega_t \times \Xi_t}\|, 10 \sqrt{\frac{p_1 p_2 p_3}{m_1 m_2 m_3}} \|Z_{t, \Omega}\|, 19 \sqrt{\frac{p_1 p_2 p_3}{p_t g_t}} \|Z_{\Xi_t}\| \right\}, \quad (29)$$

Algorithm 2 with $\lambda_t = 3\sqrt{p_t/m_t}$ yields

$$\begin{aligned} \|\hat{\mathbf{X}} - \mathbf{X}\|_{\text{HS}} &\leq C \sqrt{\frac{p_1 p_2 p_3}{m_1 m_2 m_3}} \|\mathbf{Z}_{[\Omega_1, \Omega_2, \Omega_3]}\|_{\text{HS}} + C \sqrt{p_1 p_2 p_3} \sum_{t=1}^3 \left(\frac{\|Z_{\Omega_t \times \Xi_t}\|_F}{\sqrt{g_t m_t}} + \frac{\|Z_{\Xi_t}\|_F}{\sqrt{g_t p_t}} \right), \\ \|\hat{\mathbf{X}} - \mathbf{X}\|_{\text{op}} &\leq C \sqrt{\frac{p_1 p_2 p_3}{m_1 m_2 m_3}} \|\mathbf{Z}_{[\Omega_1, \Omega_2, \Omega_3]}\|_{\text{op}} + C \sqrt{p_1 p_2 p_3} \sum_{t=1}^3 \left(\frac{\|Z_{\Omega_t \times \Xi_t}\|}{\sqrt{g_t m_t}} + \frac{\|Z_{\Xi_t}\|}{\sqrt{g_t p_t}} \right), \end{aligned}$$

with probability at least $1 - 2 \sum_{t=1}^3 r_t \{ \exp(-m_t/(16r_t\rho)) + \exp(-g_t/(64r_t\rho)) \}$.

Remark 3 The incoherence conditions (28) are widely used in matrix and tensor completion literature (see, e.g., Candès and Tao (2010); Recht (2011); Yuan and Zhang (2016)). Their conditions basically characterize every entry of X as containing a similar level of information for the whole tensor. Therefore, we should have enough knowledge to recover the original tensor based on the observable entries.

4 Simulation Study

In this section, we investigate the numerical performance of the proposed procedure in a variety of settings. We repeat each setting 1000 times and record the average relative loss in Hilbert Schmitt norm, i.e., $\|\hat{\mathbf{X}} - \mathbf{X}\|_{\text{HS}}/\|\mathbf{X}\|_{\text{HS}}$.

We first focus on the setting with i.i.d. Gaussian noise. To be specific, we randomly generate $\mathbf{X} = \mathbf{S} \times_1 E_1 \times_2 E_2 \times_3 E_3$, where $\mathbf{S} \in \mathbb{R}^{r_1 \times r_2 \times r_3}$, $E_1 \in \mathbb{R}^{p_1 \times r_1}$, $E_2 \in \mathbb{R}^{p_2 \times r_2}$, $E_3 \in \mathbb{R}^{p_3 \times r_3}$ are all with i.i.d. standard Gaussian entries. We can verify that \mathbf{X} becomes a rank- (r_1, r_2, r_3) tensor with probability 1 whenever r_1, r_2, r_3 satisfy $\max^2(r_1, r_2, r_3) \leq r_1 r_2 r_3$. Then we generate the Cross tensor measurement $\mathbf{\Omega}$ as in (3) with Ω_t including uniformly randomly selected m_t values from $[1 : p_t]$ and Ξ_t including uniformly randomly selected g_t values from $\prod_{s \neq t} \Omega_s$, and contaminate $\mathbf{X}_{\mathbf{\Omega}}$ with i.i.d. Gaussian noise: $\mathbf{Y}_{\mathbf{\Omega}} = \mathbf{X}_{\mathbf{\Omega}} + \mathbf{Z}_{\mathbf{\Omega}}$, where $Z_{ijk} \stackrel{iid}{\sim} (0, \sigma^2)$. Under such configuration, we study the influence of different factors, including $\lambda_t, \sigma, m_t, g_t, p_t$ to the numerical performance.

Under the Gaussian noise setting, we first compare different choices of tuning parameters λ_t . To be specific, set $p_1 = p_2 = p_3 = 50, m_1 = m_2 = m_3 = g_1 = g_2 = g_3 = 10, r_1 = r_2 = r_3 = 3$ and let σ range from 1 to 0.01 and λ_t range from $1.5\sqrt{p_t/m_t}$ to $4\sqrt{p_t/m_t}$, respectively. The average relative Hilbert Schmitt norm loss of $\hat{\mathbf{X}}$ from Algorithm 2 with $\lambda_t \in [1.5\sqrt{p_t/m_t}, 4\sqrt{p_t/m_t}]$ is reported in Figure 3(a). It can be seen that the average relative loss decays when the noise level is decreasing. After comparing different choices of λ_t , $3\sqrt{p_t/m_t}$ works the best under different σ , which matches our suggestion in theoretical analysis. Thus, we set $\lambda_t = 3\sqrt{p_t/m_t}$ for all the other simulation settings and real data analysis.

We also compare the effects of $m_t = |\Omega_t|$ and $g_t = |\Xi_t|$ in the numerical performance of Algorithm 2. We set $p_1 = p_2 = p_3 = 50, r_1 = r_2 = r_3 = 3, \sigma = 0.3, \lambda_t = 3\sqrt{p_t/m_t}$ and let g_t, m_t vary from 6 to 30, to plot the average relative Hilbert-Schmitt norm loss in Figure 3(b). It can be seen that as g_t, m_t grow, namely when more entries are observable, better recovery performance can be achieved.

To further study the impact of high-dimensionality to the proposed procedure, we consider the setting where the dimension of \mathbf{X} further grows. Here, $r_1 = r_2 = r_3 = 3, \sigma = 0.3, m_1 = m_2 = m_3 = g_1 = g_2 = g_3 \in \{10, 15, 20, 25\}$ and p_1, p_2, p_3 grow from 100 to 500. The average

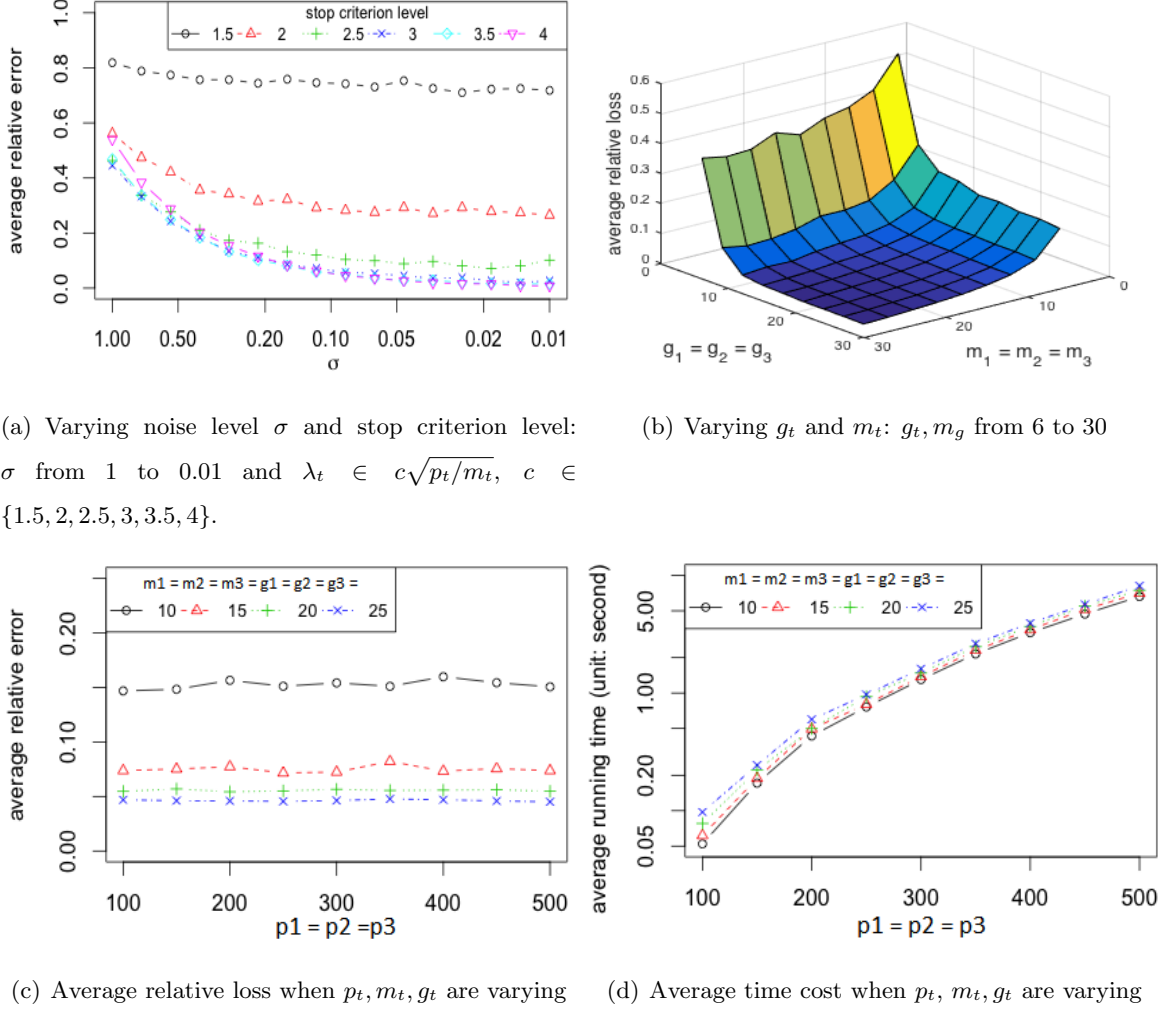
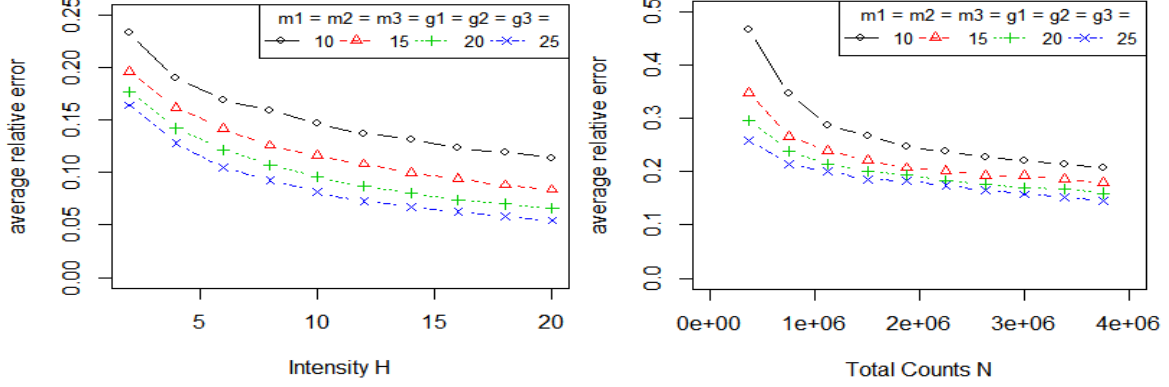


Figure 3: Numerical performance under Gaussian noise settings

relative loss in Hilbert-Schmitt norm and average running time are provided in Figure 3(c) and (d), respectively. Particularly, the recovery of 500-by-500-by-500 tensors involves 125,000,000 variables, but the proposed procedure provides stable recovery within 10 seconds on average by the PC with 3.1 GHz CPU, which demonstrates the efficiency of our proposed algorithm.

Next we move on to the setting where observations take discrete random values. High-dimensional count data commonly appear in a wide range of applications, including fluorescence microscopy, network flow, and microbiome (see, e.g., Nowak and Kolaczyk (2000); Jiang et al. (2015); Cao et al. (2016); Cao and Xie (2016), etc), where Poisson and multinomial distributions are often used in modeling the counts. In this simulation study, we generate $\mathbf{S} \in \mathbb{R}^{r_1 \times r_2 \times r_3}$, $E_t \in$



(a) Poisson model with varying m_t, g_t and intensity H (b) Multinomial model with varying m_t, g_t , total count N

Figure 4: Average relative loss in HS norm based on Poisson and multinomial observations. Here, $p_1 = p_2 = p_3 = 50, r_1 = r_2 = r_3 = 3$.

$\mathbb{R}^{p_t \times r_t}$ as absolute values of i.i.d. standard normal random variables, and calculate

$$\mathbf{X} = \frac{\mathbf{S} \times_1 E_1 \times_2 E_2 \times_3 E_3}{\sum_{i=1}^{p_1} \sum_{j=1}^{p_2} \sum_{k=1}^{p_3} (\mathbf{S} \times_1 E_1 \times_2 E_2 \times_3 E_3)_{ijk}}.$$

Ω_t, Ξ_t are generated similarly as before, $p_1 = p_2 = p_3 = 50, r_1 = r_2 = r_3 = 3, m_1 = m_2 = m_3 = g_1 = g_2 = g_3 \in \{10, 15, 20, 25\}$, and $\mathbf{Y} = (\mathbf{Y}_{ijk})$ are Poisson or multinomial distributed:

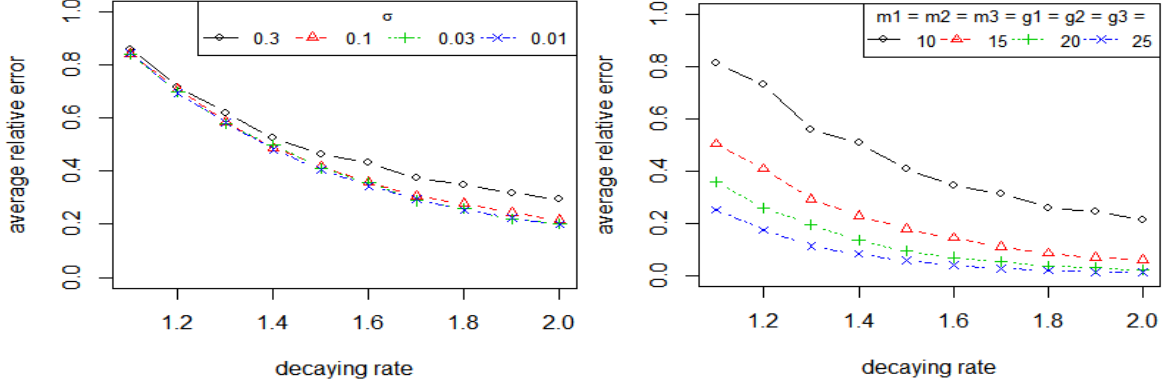
$$\mathbf{Y}_{ijk} \sim \text{Poisson}(H\mathbf{X}_{ijk}), \quad \text{or} \quad \mathbf{Y}_{ijk} \sim \text{Multinomial}(N; \mathbf{X}), (i, j, k) \in [1 : p_1, 1 : p_2, 1 : p_3].$$

Here H is a known intensity parameter in Poisson observations and N is the total count parameter in multinomial observations. As shown in Figure 4, the proposed Algorithm 2 performs stably for these two types of noisy structures.

Although \mathbf{X} is assumed to be exactly low-rank in all theoretical studies, it is not necessary in practice. In fact, our simulation study shows that Algorithm (2) performs well when \mathbf{X} is only approximately low-rank. Specifically, we fix $p_1 = p_2 = p_3 = 50$, generate $\mathbf{W} \in \mathbb{R}^{p_1 \times p_2 \times p_3}$ from i.i.d. standard normal, set $U_1 \in \mathbb{O}_{p_1}, U_2 \in \mathbb{O}_{p_2}, U_3 \in \mathbb{O}_{p_3}$ as uniform random orthogonal matrices, and $E_t = \text{diag}(1, 1, 1^{-\alpha}, \dots, (p_t - 2)^{-\alpha})$. \mathbf{X} is then constructed as

$$\mathbf{X} = \mathbf{W} \times_1 (E_1 U_1) \times_2 (E_2 U_2) \times_3 (E_3 U_3).$$

Here, α measures the decaying rate of singular values of each matricization of \mathbf{X} and \mathbf{X} becomes exactly rank-(3, 3, 3) when $\alpha = \infty$. We consider different decay rates α , noise levels σ , and



(a) Fixed $m_t = g_t = 10$, varying singular value decay- (b) Fixed $\sigma = 0.3$, varying singular value decaying
ing rate α and noise level σ . rate α and m_t, g_t .

Figure 5: Average relative loss for approximate low-rank tensors.

observation set sizes m_t and g_t . The corresponding average relative Hilbert-Schmitt norm loss is reported in Figure 5. It can be seen that although \mathbf{X} is not exactly low rank, as long as the singular values of each matricization of \mathbf{X} decay sufficiently fast, a desirable completion of \mathbf{X} can still be achieved. It can be seen from Figure 5 that, although \mathbf{X} is assumed to be exactly low-rank in theoretical analysis, such an assumption is not necessary in practice if the singular values of each matricizations decay sufficiently fast, which again demonstrates the robustness of the proposed procedure.

5 Real Data Illustration

In this section, we apply the proposed Cross tensor measurements scheme to a real dataset on attention hyperactivity disorder (ADHD) available from ADHD-200 Sample Initiative (http://fcon_1000.projects.nitrc.org/indi/adhd200/). ADHD is a common disease that affects at least 5-7% of school-age children and may accompany patients throughout their life with direct costs of at least \$36 billion per year in the United States. Despite being the most common mental disorder in children and adolescents, the cause of ADHD is largely unclear. To investigate the disease, the ADHD-200 study covered 285 subjects diagnosed with ADHD and 491 control subjects. After data cleaning, the dataset contains 776 tensors of dimension 121-by-145-by-121:

$\mathbf{Y}_i, i = 1, \dots, 776$. The storage space for these data through naive format is $121 \times 145 \times 121 \times 776 \times 4\text{B} \approx 6.137 \text{ GB}$, which makes it difficult and costly for sampling, storage and computation. Therefore, we hope to reduce the sampling size for ADHD brain imaging data via the proposed Cross tensor measurement scheme.

Figure 6 shows the singular values of each matricization of a randomly selected \mathbf{Y}_i . We can see that \mathbf{Y}_i is approximately Tucker low-rank.

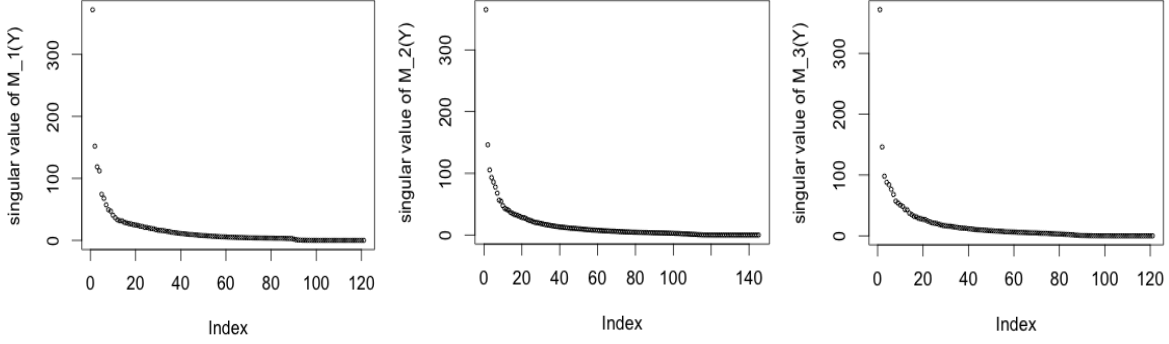


Figure 6: Singular value decompositions for each matricization of \mathbf{Y}

Similar to previous simulation settings, we uniformly randomly select $\Omega_t \subseteq [1 : p_t]$, $\Xi_t \subseteq \prod_{s \neq t} \Omega_s$ such that $|\Omega_t| = m_t$, $|\Xi_t| = g_t$. Particularly, we choose $m_t = \text{round}(\rho \cdot p_t)$, $g_t = \text{round}(m_1 m_2 m_3 / p_t)$, where ρ varies from 0.1 to 0.5 and $\text{round}(\cdot)$ is the function that rounds its input to the nearest integer. After observing partial entries of each tensor, we apply Algorithm 2 with $\lambda_t = 3\sqrt{p_t/m_t}$ to obtain $\hat{\mathbf{X}}$. Different from some of the previous studies (e.g. Zhou et al. (2013)), our algorithm is adaptive and tuning-free so that we do not need to subjectively specify the rank of the target tensors beforehand.

Suppose $\text{rank}(\hat{\mathbf{X}}) = (\hat{r}_1, \hat{r}_2, \hat{r}_3)$, $\hat{U}_1 \in \mathbb{O}_{p_1, \hat{r}_1}$, $\hat{U}_2 \in \mathbb{O}_{p_2, \hat{r}_2}$, $\hat{U}_3 \in \mathbb{O}_{p_3, \hat{r}_3}$ are the left singular vectors of $\mathcal{M}_1(\hat{\mathbf{X}})$, $\mathcal{M}_2(\hat{\mathbf{X}})$, $\mathcal{M}_3(\hat{\mathbf{X}})$, respectively. We are interested in investigating the performance of $\hat{\mathbf{X}}$, but the absence of the true tank of the underlying tensor \mathbf{X} makes it difficult to directly compare $\hat{\mathbf{X}}$ and \mathbf{X} . Instead, we compare $\hat{\mathbf{X}}$ with $\tilde{\mathbf{X}}$, where $\tilde{\mathbf{X}}$ is the rank- $(\hat{r}_1, \hat{r}_2, \hat{r}_3)$ tensor obtained through the high-order singular value decomposition (HOSVD) (see e.g. Kolda and Bader (2009)) based on all observations in \mathbf{Y} :

$$\tilde{\mathbf{X}} = \mathbf{Y} \times_1 \mathbb{P}_{\tilde{U}_1} \times_2 \mathbb{P}_{\tilde{U}_2} \times_3 \mathbb{P}_{\tilde{U}_3}. \quad (30)$$

Here $\tilde{U}_1 \in \mathbb{O}_{p_1, r_1}, \tilde{U}_2 \in \mathbb{O}_{p_2, r_2}, \tilde{U}_3 \in \mathbb{O}_{p_3, r_3}$ are the first r_1, r_2 and r_3 left singular vectors of $\mathcal{M}_1(\mathbf{Y}), \mathcal{M}_2(\mathbf{Y})$ and $\mathcal{M}_3(\mathbf{Y})$, respectively. Particularly, we compare $\|\hat{\mathbf{X}} - \mathbf{Y}\|_{\text{HS}}$ and $\|\tilde{\mathbf{X}} - \mathbf{Y}\|_{\text{HS}}$,

	Sampling Ratio (See (6))	$\frac{\ \hat{\mathbf{X}} - \mathbf{Y}\ _{\text{HS}}}{\ \tilde{\mathbf{X}} - \mathbf{Y}\ _{\text{HS}}}$	$\frac{1}{\sqrt{\hat{r}_1}} \ \hat{U}_1^\top \tilde{U}_1\ _F$	$\frac{1}{\sqrt{\hat{r}_2}} \ \hat{U}_2^\top \tilde{U}_2\ _F$	$\frac{1}{\sqrt{\hat{r}_3}} \ \hat{U}_3^\top \tilde{U}_3\ _F$
$m_t = \text{round}(.1p_t)$	0.0035	1.5086	0.8291	0.8212	0.8318
$m_t = \text{round}(.2p_t)$	0.0267	1.2063	0.9352	0.9110	0.9155
$m_t = \text{round}(.3p_t)$	0.0832	1.0918	0.9650	0.9571	0.9634
$m_t = \text{round}(.4p_t)$	0.1766	1.0506	0.9769	0.9745	0.9828
$m_t = \text{round}(.5p_t)$	0.3066	1.0312	0.9832	0.9840	0.9905

Table 1: Comparison between $\hat{\mathbf{X}}$ and $\tilde{\mathbf{X}}$ for ADHD brain imaging data.

i.e. the rank- (r_1, r_2, r_3) approximation based on limited number of Cross tensor measurements and the approximation based on all measurements. We also compare $\hat{U}_1, \hat{U}_2, \hat{U}_3$ and $\tilde{U}_1, \tilde{U}_2, \tilde{U}_3$ by calculating $\frac{1}{\sqrt{\hat{r}_t}} \|\hat{U}_t^\top \tilde{U}_t\|_F$. The study is performed on 10 randomly selected images and repeated 100 times for each of them. We can immediately see from the result in Table 1 that on average, $\|\hat{\mathbf{X}} - \mathbf{Y}\|_{\text{HS}}$, i.e. rank- (r_1, r_2, r_3) approximation error with limited numbers of Cross tensor measurements, can get very close to $\|\tilde{\mathbf{X}} - \mathbf{Y}\|_{\text{HS}}$, i.e. rank- (r_1, r_2, r_3) approximation error with the whole tensor \mathbf{Y} . Besides, $\frac{1}{\sqrt{\hat{r}_t}} \|\hat{U}_t^\top \tilde{U}_t\|_F$ is close to 1, which means the singular vectors calculated from limited numbers of Cross tensor measurements are not too far from the ones calculated from the whole tensor.

Therefore, by the proposed Cross Tensor Measurement Scheme and a small fraction of observable entries, we can approximate the leading principle component of the original tensor just as if we have observed all voxels. This illustrates the power of the proposed algorithm.

Acknowledgments

The author would like to thank Lexin Li for sharing the ADHD dataset and helpful discussion.

6 Proofs

We collect the proofs of the main results (Theorems 1 and 2) in this section. The proofs for other results are postponed to the supplementary materials.

6.1 Proof of Theorem 1.

First, we shall note that $\mathbf{Y} = \mathbf{X}$ in the exact low-rank and noiseless setting. For each $t = 1, 2, 3$, according to definitions, X_{Ξ_t} is a collection of columns of $\mathcal{M}_t(\mathbf{X})$ and $X_{\Omega_t \times \Xi_t}$ is a collection of rows of X_{Ξ_t} . Then we have $\text{rank}(X_{\Omega_t \times \Xi_t}) \leq \text{rank}(X_{\Xi_t}) \leq \text{rank}(\mathcal{M}_t(\mathbf{Y}))$. Given the assumptions, we have $\text{rank}(X_{\Omega_t \times \Xi_t}) = \text{rank}(\mathcal{M}_t(\mathbf{X})) = r_t$. Thus,

$$\text{rank}(X_{\Omega_t \times \Xi_t}) = \text{rank}(X_{\Xi_t}) = \text{rank}(\mathcal{M}_t(\mathbf{X})) = r_t.$$

Then $\mathcal{M}_t(\mathbf{X})$ and X_{Ξ_t} share the same column subspace and there exists a matrix $W_t \in \mathbb{R}^{g_t \times \prod_{s \neq t} p_s}$ such that $\mathcal{M}_t(\mathbf{X}) = X_{\Xi_t} \cdot W_t$. On the other hand, since X_{Ξ_t} and $X_{\Omega_t \times \Xi_t}$ have the same row subspace, we have

$$X_{\Xi_t} = X_{\Xi_t} \cdot (X_{\Omega_t \times \Xi_t})^\dagger \cdot X_{\Omega_t \times \Xi_t} = R_t \cdot X_{\Omega_t \times \Xi_t}. \quad (31)$$

Additionally, X_{Ξ_t} and $X_{\Omega_t \times \Xi_t}$ can be factorized as $X_{\Xi_t} = P_1 Q$, $X_{\Omega_t \times \Xi_t} = P_2 Q$, where $P_1 \in \mathbb{R}^{p_t \times r_t}$, $P_2 \in \mathbb{R}^{m_t \times r_t}$, $Q \in \mathbb{R}^{r_t \times g_t}$ and $\text{rank}(P_1) = \text{rank}(P_2) = \text{rank}(Q) = r_t$. In this case, for any matrices $\tilde{M} \in \mathbb{R}^{m_t \times r_t}$, $\tilde{N} \in \mathbb{R}^{g_t \times r_t}$ with $\text{rank}(\tilde{M}^\top X_{\Omega_t \times \Xi_t} \tilde{N}) = r_t$, we have

$$\begin{aligned} \tilde{R}_t \cdot X_{\Omega_t \times \Xi_t} &= X_{\Xi_t} \tilde{N} \left(\tilde{M}^\top X_{\Omega_t \times \Xi_t} \tilde{N} \right)^{-1} \tilde{M}^\top \cdot X_{\Omega_t \times \Xi_t} = P_1 Q \tilde{N} \left(\tilde{M}^\top P_2 Q \tilde{N} \right)^{-1} \tilde{M}^\top P_2 Q \\ P_1 Q \tilde{N} (Q \tilde{N})^{-1} (\tilde{M}^\top P_2)^{-1} \tilde{M}^\top P_2 Q &= P_1 Q = X_{\Xi_t}. \end{aligned} \quad (32)$$

Right multiplying W_t to (31) and (32), we obtain

$$\begin{aligned} \mathcal{M}_t(\mathbf{X}) &= X_{\Xi_t} \cdot W_t = R_t \cdot X_{\Omega_t \times \Xi_t} \cdot W_t = R_t \cdot (\mathcal{M}_t(\mathbf{Y}))_{[\Omega_t, :]}, \\ &= \tilde{R}_t \cdot X_{\Omega_t \times \Xi_t} \cdot W_t = \tilde{R}_t \cdot (\mathcal{M}_t(\mathbf{Y}))_{[\Omega_t, :]}. \end{aligned}$$

By folding $\mathcal{M}_t(\mathbf{X})$ back to the tensors and Lemma 3, we obtain

$$\begin{aligned} \mathbf{X} &= \mathbf{X}_{[\Omega_1, :, :]} \times_1 R_1 = \mathbf{X}_{[:, \Omega_2, :]} \times_2 R_2 = \mathbf{X}_{[:, :, \Omega_3]} \times_3 R_3 \\ &= \mathbf{X}_{[\Omega_1, :, :]} \times_1 \tilde{R}_1 = \mathbf{X}_{[:, \Omega_2, :]} \times_2 \tilde{R}_2 = \mathbf{X}_{[:, :, \Omega_3]} \times_3 \tilde{R}_3. \end{aligned}$$

By the equation above,

$$\begin{aligned}\mathbf{X}_{[\Omega_1, \Omega_2, \Omega_3]} \times_1 R_1 &= \mathbf{X}_{[\Omega_1, \Omega_2, \Omega_3]} \times_1 \tilde{R}_1 = \mathbf{X}_{[:, \Omega_2, \Omega_3]}, \\ \mathbf{X}_{[:, \Omega_2, \Omega_3]} \times_2 R_2 &= \mathbf{X}_{[:, \Omega_2, \Omega_3]} \times_2 \tilde{R}_2 = \mathbf{X}_{[:, :, \Omega_3]}, \quad \mathbf{X}_{[:, :, \Omega_3]} \times_3 R_3 = \mathbf{X}_{[:, :, \Omega_3]} \times_3 \tilde{R}_3 = \mathbf{X}.\end{aligned}$$

Therefore,

$$\mathbf{X}_{[\Omega_1, \Omega_2, \Omega_3]} \times_1 R_1 \times_2 R_2 \times_3 R_3 = \mathbf{X}_{[\Omega_1, \Omega_2, \Omega_3]} \times_1 \tilde{R}_1 \times_2 \tilde{R}_2 \times_3 \tilde{R}_3 = \mathbf{X},$$

which concludes the proof of Theorem 1. \square

6.2 Proof of Theorem 2.

Based on the proof for Theorem 1, we know

$$\mathbf{X} = \mathbf{X}_{[\Omega_1, \Omega_2, \Omega_3]} \times_1 \tilde{R}_1 \times_2 \tilde{R}_2 \times_3 \tilde{R}_3,$$

where

$$\tilde{R}_t = X_{\Xi_t} \tilde{N} \left(\tilde{M}^\top X_{\Omega_t \times \Xi_t} \tilde{N} \right)^{-1} \tilde{M}^\top \in \mathbb{R}^{p_t \times m_t}, \quad (33)$$

for any $\tilde{M} \in \mathbb{R}^{m_t \times r_t}$, $\tilde{N} \in \mathbb{R}^{g_t \times r_t}$ satisfying $\tilde{M}^\top X_{\Omega_t \times \Xi_t} \tilde{N}$ is non-singular. The proof for Theorem 2 is relatively long. For better presentation, we divide the proof into steps. Before going into detailed discussions, we list all notations with the definitions and possible simple explanations in Table 2 in the supplementary materials.

1. Denote

$$\begin{aligned}\hat{N}_t, N_t &\in \mathbb{O}_{g_t, r_t} \text{ as the first } r_t \text{ right singular vectors of } Y_{\Xi_t} \text{ and } X_{\Xi_t}, \text{ respectively;} \\ \hat{M}_t, M_t &\in \mathbb{O}_{m_t, r_t} \text{ as the first } r_t \text{ left singular vectors of } Y_{t, \Omega} \text{ and } X_{t, \Omega}, \text{ respectively.}\end{aligned} \quad (34)$$

It is easy to see that alternate characterization for \hat{N}_t and \hat{M}_t are

$$\hat{N}_t = V_{[:, 1:r_t]}^{(A)}, \quad \hat{M}_t = U_{[:, 1:r_t]}^{(B)}. \quad (35)$$

Denote $\tau = 1/5$. In this step, we prove that \hat{M}_t, M_t ; \hat{N}_t, N_t are close by providing the upper bounds on singular subspace perturbations,

$$\|\sin \Theta(\hat{M}_t, M_t)\| \leq \tau^2/(1 - 2\tau), \quad \|\sin \Theta(\hat{N}_t, N_t)\| \leq \tau^2/(1 - 2\tau); \quad (36)$$

as well as the inequality which ensures that J_t is bounded away from being singular,

$$\begin{aligned}\sigma_{\min}(\hat{M}_t^\top X_{\Omega_t \times \Xi_t} \hat{N}_t) &\geq (1 - \tau^4/(1 - 2\tau)^2) \sigma_{\min}(X_{\Omega_t \times \Xi_t}), \\ \sigma_{\min}(\hat{M}_t^\top Y_{\Omega_t \times \Xi_t} \hat{N}_t) &\geq (1 - \tau^4/(1 - 2\tau)^2 - \tau) \sigma_{\min}(X_{\Omega_t \times \Xi_t}).\end{aligned}\tag{37}$$

Actually, based on Assumption (20), we have

$$\sigma_{r_t}(Y_{\Xi_t} N_t) \geq \sigma_{r_t}(X_{\Xi_t} N_t) - \|Z_{\Xi_t} N_t\| \geq \sigma_{r_t}(X_{\Xi_t}) - \tau \sigma_{r_t}(X_{\Xi_t}) = (1 - \tau) \sigma_{r_t}(A_{\Xi_t});$$

$$\sigma_{r_t+1}(X_{\Xi_t}) \leq \sigma_{r_t+1}(X_{\Xi_t}) + \|Z_{\Xi_t}\| \leq \tau \sigma_{r_t}(A_{\Xi_t});$$

$$\left\| \mathbb{P}_{X_{\Xi_t} N_t} X_{\Xi_t}(N_t)_\perp \right\| \leq \|X_{\Xi_t}(N_t)_\perp\| = \|A_{\Xi_t}(N_t)_\perp + Z_{\Xi_t}(N_t)_\perp\| \leq \|Z_{\Xi_t}\| \leq \tau \sigma_{r_t}(A_{\Xi_t}).$$

Here $(N_t)_\perp$ is the orthogonal complement matrix, i.e. $[N_t \ (N_t)_\perp] \in \mathbb{O}_{g_t}$. By setting $A = X_{\Xi_t}$, $W = N_t$ in the scenario of the unilateral perturbation bound (Proposition 1 in Cai and Zhang (2016)), we then obtain

$$\left\| \sin \Theta(\hat{N}_t, N_t) \right\| \leq \frac{\sigma_{r_t+1}(X_{\Xi_t}) \left\| \mathbb{P}_{(X_{\Xi_t} N_t)} Z_{\Xi_t}(N_t)_\perp \right\|}{\sigma_{r_t}^2(X_{\Xi_t} N_t) - \sigma_{r_t+1}^2(X_{\Xi_t})} \leq \frac{\tau \cdot \tau}{(1 - \tau)^2 - \tau^2} = \tau^2/(1 - 2\tau).$$

Here $\|\sin \Theta(\cdot, \cdot)\|$ is a commonly used distance between orthogonal subspaces. Similarly, based on the assumption that $\tau \sigma_{r_t}(A_{t,\Omega}) \geq \|Z_{t,\Omega}\|$, we can derive

$$\left\| \sin \Theta(\hat{M}_t, M_t) \right\| \leq \tau^2/(1 - 2\tau),$$

which proves (36). Based on the property for $\sin \Theta$ distance (Lemma 1 in Cai and Zhang (2016)),

$$\begin{aligned}\sigma_{\min}(\hat{N}_t^\top N_t) &= \sqrt{1 - \|\sin \Theta(\hat{N}_t, N_t)\|^2} \geq \sqrt{1 - \tau^4/(1 - 2\tau)^2}; \\ \sigma_{\min}(\hat{M}_t^\top M_t) &= \sqrt{1 - \|\sin \Theta(\hat{M}_t, M_t)\|^2} \geq \sqrt{1 - \tau^4/(1 - 2\tau)^2}.\end{aligned}$$

Also, since M_t, N_t coincide with the left and right singular subspaces of $X_{\Omega_t \times \Xi_t}$ respectively, we have

$$\begin{aligned}\sigma_{\min}(\hat{M}_t^\top X_{\Omega_t \times \Xi_t} \hat{N}_t) &= \sigma_{\min}(\hat{M}_t^\top \mathbb{P}_{M_t} X_{\Omega_t \times \Xi_t} \mathbb{P}_{N_t} \hat{N}_t) = \sigma_{\min}(\hat{M}_t^\top M_t M_t^\top X_{\Omega_t \times \Xi_t} N_t N_t^\top \hat{N}_t) \\ &\geq \sigma_{\min}(\hat{M}_t^\top M_t) \sigma_{\min}(M_t^\top X_{\Omega_t \times \Xi_t} N_t) \sigma_{\min}(N_t^\top \hat{N}_t) \geq (1 - \tau^4/(1 - \tau)^2) \sigma_{\min}(X_{\Omega_t \times \Xi_t}) \\ \sigma_{\min}(\hat{M}_t^\top Y_{\Omega_t \times \Xi_t} \hat{N}_t) &\geq \sigma_{\min}(\hat{M}_t^\top X_{\Omega_t \times \Xi_t} \hat{N}_t) - \|Z_{\Omega_t \times \Xi_t}\| \geq (1 - \tau^4/(1 - 2\tau)^2 - \tau) \sigma_{\min}(X_{\Omega_t \times \Xi_t}),\end{aligned}$$

which has finished the proof for (37).

2. In this step, we prove that under the given setting, $\hat{r}_t \geq r_t$ for $t = 1, 2, 3$. We only need to show that for each $t = 1, 2, 3$, the stopping criterion holds when $s = r_t$, i.e.

$$\left\| (A_t)_{[:,1:r_t]} (J_t)_{[1:r_t,1:r_t]}^{-1} \right\| \leq \lambda_t. \quad (38)$$

According to the definitions in (16), A_t, J_t and \hat{M}_t, \hat{N}_t can be related as

$$\begin{aligned} (A_t)_{[:,1:r_t]} &= Y_{\Xi_t} V_{[:,1:r_t]}^{(A)} \stackrel{(35)}{=} Y_{\Xi_t} \hat{N}_t = (X_{\Xi_t} + Z_{\Xi_t}) \hat{N}_t, \\ (J_t)_{[1:r_t,1:r_t]} &= (U_{[:,1:r_t]}^{(B)})^\top Y_{\Omega_t \times \Xi_t} V_{[:,1:r_t]}^{(A)} \stackrel{(35)}{=} \hat{M}_t^\top Y_{\Omega_t \times \Xi_t} \hat{N}_t = \hat{M}_t^\top (X_{\Omega_t \times \Xi_t} + Z_{\Omega_t \times \Xi_t}) \hat{N}_t. \end{aligned}$$

Therefore, in order to show (38), we only need to prove that $\hat{M}_t^\top Y_{\Omega_t \times \Xi_t} \hat{N}_t$ is non-singular and

$$\left\| (X_{\Xi_t} + Z_{\Xi_t}) \hat{N}_t \cdot \left(\hat{M}_t^\top (X_{\Omega_t \times \Xi_t} + Z_{\Omega_t \times \Xi_t}) \hat{N}_t \right)^{-1} \right\| \leq \lambda_t. \quad (39)$$

Recall that $U_t \in \mathbb{O}_{p_t, r_t}$ is the singular subspace for $\mathcal{M}_t(\mathbf{X})$, so there exists another matrix $Q \in \mathbb{R}^{r_t \times g_t}$ such that X_{Ξ_t} , a set of columns of $\mathcal{M}_t(\mathbf{X})$, can be written as

$$X_{\Xi_t} = U_t \cdot Q, \quad \text{then} \quad X_{\Omega_t \times \Xi_t} = U_{t, \Omega} \cdot Q. \quad (40)$$

Here $U_{t, \Omega} = (U_t)_{[\Omega_t, :]}$ is a collection of rows from U_t , and

$$X_{\Xi_t} X_{\Omega_t \times \Xi_t}^\dagger = U_t Q (U_{t, \Omega} Q)^\dagger = U_t U_{t, \Omega}^\dagger, \quad \text{then} \quad \left\| X_{\Xi_t} X_{\Omega_t \times \Xi_t}^\dagger \right\| = \sigma_{\min}^{-1}(U_{t, \Omega}).$$

For convenience, we denote

$$\bar{\lambda}_t = \frac{1}{\sigma_{\min}(U_{t, \Omega})} = \left\| X_{\Xi_t} X_{\Omega_t \times \Xi_t}^\dagger \right\| \stackrel{(22)}{\leq} \frac{1}{2} \lambda_t. \quad (41)$$

In this case,

$$\begin{aligned} & \left\| X_{\Xi_t} \hat{N}_t (\hat{M}_t^\top X_{\Omega_t \times \Xi_t} \hat{N}_t)^{-1} \right\| = \left\| U_t Q \hat{N}_t (\hat{M}_t^\top U_{t, \Omega} Q \hat{N}_t)^{-1} \right\| \\ &= \left\| U_t \left(\hat{M}_t^\top U_{t, \Omega} \right)^{-1} \right\| = \left\| \left(\hat{M}_t^\top U_{t, \Omega} \right)^{-1} \right\| \leq \frac{1}{\sigma_{\min}(U_{t, \Omega})} = \bar{\lambda}_t. \end{aligned} \quad (42)$$

Furthermore,

$$\sigma_{r_t}(X_{\Omega_t \times \Xi_t}) = \sigma_{\min}(U_{t, \Omega} \cdot Q) \geq \sigma_{\min}(U_{t, \Omega}) \cdot \sigma_{\min}(Q) = \sigma_{\min}(U_{t, \Omega}) \cdot \sigma_{\min}(U_t Q) = \sigma_{\min}(U_{t, \Omega}) \cdot \sigma_{r_t}(X_{\Xi_t}). \quad (43)$$

Therefore,

$$\begin{aligned}
& \left\| (X_{\Xi_t} + Z_{\Xi_t}) \hat{N}_t \cdot \left(\hat{M}_t^\top (X_{\Omega_t \times \Xi_t} + Z_{\Omega_t \times \Xi_t}) \hat{N}_t \right)^{-1} \right\| \\
& \leq \left\| X_{\Xi_t} \hat{N}_t \cdot \left(\hat{M}_t^\top (X_{\Omega_t \times \Xi_t} + Z_{\Omega_t \times \Xi_t}) \hat{N}_t \right)^{-1} \right\| + \left\| Z_{\Xi_t} \hat{N}_t \cdot \left(\hat{M}_t^\top (X_{\Omega_t \times \Xi_t} + Z_{\Omega_t \times \Xi_t}) \hat{N}_t \right)^{-1} \right\| \\
& \stackrel{\text{Lemma 5}}{\leq} \left\| X_{\Xi_t} \hat{N}_t \cdot \left(\hat{M}_t^\top X_{\Omega_t \times \Xi_t} \hat{N}_t \right)^{-1} \left(\hat{M}_t^\top Z_{\Omega_t \times \Xi_t} \hat{N}_t \right) \left(\hat{M}_t^\top (X_{\Omega_t \times \Xi_t} + Z_{\Omega_t \times \Xi_t}) \hat{N}_t \right)^{-1} \hat{M}_t \right\| \\
& \quad + \left\| X_{\Xi_t} \hat{N}_t \cdot \left(\hat{M}_t^\top X_{\Omega_t \times \Xi_t} \hat{N}_t \right)^{-1} \right\| + \frac{\|Z_{\Xi_t}\|}{\sigma_{\min}(\hat{M}_t^\top Y_{\Omega_t \times \Xi_t} \hat{N}_t)} \\
& \stackrel{(37)(42)}{\leq} \bar{\lambda}_t + \bar{\lambda}_t \frac{\|Z_{\Omega_t \times \Xi_t}\|}{(1 - \tau^4/(1 - 2\tau)^2 - \tau) \sigma_{\min}(X_{\Omega_t \times \Xi_t})} + \frac{\|Z_{\Xi_t}\|}{(1 - \tau^4/(1 - 2\tau)^2 - \tau) \sigma_{\min}(X_{\Omega_t \times \Xi_t})} \\
& \stackrel{(20)}{\leq} \bar{\lambda}_t + \frac{\bar{\lambda}_t \tau}{1 - \tau^4/(1 - 2\tau)^2 - \tau} + \frac{\tau \sigma_{r_t}(X_{\Xi_t})}{(1 - \tau^4/(1 - 2\tau)^2 - \tau) \sigma_{\min}(X_{\Omega_t \times \Xi_t})} \\
& \stackrel{(43)}{\leq} \bar{\lambda}_t \left(1 + \frac{2\tau}{1 - \tau^4/(1 - 2\tau)^2 - \tau} \right) \stackrel{(41)}{\leq} \lambda_t,
\end{aligned}$$

which has proved our claim that $\hat{r}_t \geq r_t$ for $t = 1, 2, 3$.

3. In this step, we provide an important decomposition of $\hat{\mathbf{X}}$ under the scenario that $\hat{r}_t \geq r_t$. One major difficulty is measuring the difference between $J_{t,[1:\hat{r}_t, 1:\hat{r}_t]}^{-1}$ and $J_{t,[1:r_t, 1:r_t]}^{-1}$. For convenience, we further introduce the following notations,

$$J_{\hat{r}_t} \in \mathbb{R}^{\hat{r}_t \times \hat{r}_t}, \quad J_{\hat{r}_t} := J_{t,[1:\hat{r}_t, 1:\hat{r}_t]} = U_{t,[1:\hat{r}_t]}^{(B)\top} Y_{\Omega_t \times \Xi_t} V_{t,[1:\hat{r}_t]}^{(A)}, \quad (44)$$

$$J_{\hat{r}_t}^{(X)} := U_{t,[1:\hat{r}_t]}^{(B)\top} X_{\Omega_t \times \Xi_t} V_{t,[1:\hat{r}_t]}, \quad J_{\hat{r}_t}^{(Z)} := U_{t,[1:\hat{r}_t]}^{(B)\top} Z_{\Omega_t \times \Xi_t} V_{t,[1:\hat{r}_t]}, \quad \text{then} \quad J_{\hat{r}_t} = J_{\hat{r}_t}^{(X)} + J_{\hat{r}_t}^{(Z)}. \quad (45)$$

$$A_{\hat{r}_t} \in \mathbb{R}^{p_t \times \hat{r}_t}, \quad A_{\hat{r}_t} := A_{t,[1:\hat{r}_t]} = Y_{\Xi_t} V_{t,[1:\hat{r}_t]}^{(A)}, \quad (46)$$

$$A_{\hat{r}_t}^{(X)} := X_{\Xi_t} V_{t,[1:\hat{r}_t]}^{(A)}, \quad A_{\hat{r}_t}^{(Z)} := Z_{\Xi_t} V_{t,[1:\hat{r}_t]}^{(A)}, \quad \text{then} \quad A_{\hat{r}_t} = A_{\hat{r}_t}^{(X)} + A_{\hat{r}_t}^{(Z)}. \quad (47)$$

Let the singular value decompositions of $J_{\hat{r}_t}$ be

$$J_{\hat{r}_t} = K_t \Lambda_t L_t^\top = \begin{bmatrix} K_{t1} & K_{t2} \end{bmatrix} \cdot \begin{bmatrix} \Lambda_{t1} & \\ & \Lambda_{t2} \end{bmatrix} \cdot \begin{bmatrix} L_{t1}^\top \\ L_{t2}^\top \end{bmatrix}, \quad t = 1, 2, 3. \quad (48)$$

Here $K_t, L_t \in \mathbb{O}_{\hat{r}_t}$, $K_{t1}, L_{t1} \in \mathbb{O}_{\hat{r}_t, r_t}$, $K_{t2}, L_{t2} \in \mathbb{O}_{\hat{r}_t, r_t}$ are the singular vectors, $\Lambda_t \in \mathbb{R}^{\hat{r}_t \times \hat{r}_t}$, $\Lambda_{t1} \in \mathbb{R}^{r_t \times r_t}$ and $\Lambda_{t2} \in \mathbb{R}^{(\hat{r}_t - r_t) \times (\hat{r}_t - r_t)}$ are the singular values. Based on these SVDs, we can

correspondingly decompose \bar{R}_t (defined in (18)) as

$$\begin{aligned}
\bar{R}_t &= A_{t,[:,1:\hat{r}_t]} J_{\hat{r}_t}^{-1} U_{t,[:,1:\hat{r}_t]}^{(B)} = A_{t,[:,1:\hat{r}_t]} \left(K_{t1} \Lambda_{t1} L_{t1}^\top + K_{t2} \Lambda_{t2} L_{t2}^\top \right)^{-1} U_{t,[:,1:\hat{r}_t]}^{(B)} \\
&= A_{t,[:,1:\hat{r}_t]} \left(L_{t1} \Lambda_{t1}^{-1} K_{t1}^\top + L_{t2} \Lambda_{t2}^{-1} K_{t2}^\top \right) U_{t,[:,1:\hat{r}_t]}^{(B)} \\
&= A_{t,[:,1:\hat{r}_t]} L_{t1} \Lambda_{t1}^{-1} K_{t1}^\top U_{t,[:,1:\hat{r}_t]}^{(B)} + A_{t,[:,1:\hat{r}_t]} L_{t2} \Lambda_{t2}^{-1} K_{t2}^\top U_{t,[:,1:\hat{r}_t]}^{(B)} \\
&= Y_{\Xi_t} V_{t,[:,1:\hat{r}_t]}^{(A)} L_{t1} \left(K_{t1}^\top J_{\hat{r}_t} L_{t1} \right)^{-1} K_{t1}^\top U_{t,[:,1:\hat{r}_t]}^{(B)} \\
&\quad + Y_{\Xi_t} V_{t,[:,1:\hat{r}_t]}^{(A)} L_{t2} \left(K_{t2}^\top J_{\hat{r}_t} L_{t2} \right)^{-1} K_{t2}^\top U_{t,[:,1:\hat{r}_t]}^{(B)}.
\end{aligned} \tag{49}$$

Here, the first term above associated with $K_{t1}, L_{t1} \dots$ stands for the major part in \bar{R}_t while the second associated with K_{t2}, L_{t2} stands for the minor part. Based on this decomposition, we introduce the following notations: for any $t = 1, 2, 3$ (indicating Mode-1, 2 or 3) and $s = 1, 2$ (indicating the major or minor parts),

$$A_{ts}^{(X)} := A_{\hat{r}_t}^{(X)} L_{ts} = X_{\Xi_t} V_{t,[:,1:\hat{r}_t]}^{(A)} L_{ts}, \quad A_{ts}^{(Z)} := A_{\hat{r}_s}^{(Z)} L_{ts} = Z_{\Xi_t} V_{t,[:,1:\hat{r}_t]}^{(A)} L_{ts} \tag{50}$$

$$A_{ts} := A_{\hat{r}_t} L_{ts} = Y_{\Xi_t} V_{t,[:,1:\hat{r}_t]}^{(A)} L_{ts} = A_{ts}^{(X)} + A_{ts}^{(Z)}. \tag{51}$$

$$J_{ts}^{(X)} := K_{ts}^\top J_{\hat{r}_t} L_{ts} = K_{ts}^\top J_{\hat{r}_t}^{(X)} L_{ts} = K_{ts}^\top U_{t,[:,1:\hat{r}_t]}^{(B)\top} X_{\Omega_t \times \Xi_t} V_{t,[:,1:\hat{r}_t]}^{(A)} L_{ts}, \tag{52}$$

$$\begin{aligned}
J_{ts}^{(Z)} &:= K_{ts}^\top J_{\hat{r}_t} L_{ts} = K_{ts}^\top A_{\hat{r}_t} L_{ts} = K_{ts}^\top J_{\hat{r}_t}^{(A)} L_{ts} = K_{ts}^\top U_{t,[:,1:\hat{r}_t]}^{(B)\top} Z_{\Omega_t \times \Xi_t} V_{t,[:,1:\hat{r}_t]}^{(A)} L_{ts}, \\
J_{ts} &:= J_{ts}^{(X)} + J_{ts}^{(Z)} = K_{ts}^\top U_{t,[:,1:\hat{r}_t]}^{(B)\top} Y_{\Omega_t \times \Xi_t} V_{t,[:,1:\hat{r}_t]}^{(A)} L_{ts}.
\end{aligned} \tag{53}$$

Also, for $s_1, s_2, s_3 \in \{1, 2\}^3$, we define the projected body measurements

$$\mathbf{B}_{s_1 s_2 s_3}^{(X)} = \mathbf{X}_{[\Omega_1, \Omega_2, \Omega_3]} \times_1 \left(K_{1s_1}^\top U_{1,[1:\hat{r}_1]}^{(B)} \right) \times_2 \left(K_{2s_2}^\top U_{2,[1:\hat{r}_2]}^{(B)} \right) \times_3 \left(K_{3s_3}^\top U_{3,[1:\hat{r}_3]}^{(B)} \right) \tag{54}$$

$$\mathbf{B}_{s_1 s_2 s_3}^{(Z)} = \mathbf{Z}_{[\Omega_1, \Omega_2, \Omega_3]} \times_1 \left(K_{1s_1}^\top U_{1,[1:\hat{r}_1]}^{(B)} \right) \times_2 \left(K_{2s_2}^\top U_{2,[1:\hat{r}_2]}^{(B)} \right) \times_3 \left(K_{3s_3}^\top U_{3,[1:\hat{r}_3]}^{(B)} \right) \tag{55}$$

$$\mathbf{B}_{s_1 s_2 s_3} = \mathbf{Y}_{[\Omega_1, \Omega_2, \Omega_3]} \times_1 \left(K_{1s_1}^\top U_{1,[1:\hat{r}_1]}^{(B)} \right) \times_2 \left(K_{2s_2}^\top U_{2,[1:\hat{r}_2]}^{(B)} \right) \times_3 \left(K_{3s_3}^\top U_{3,[1:\hat{r}_3]}^{(B)} \right) = \mathbf{B}_{s_1 s_2 s_3}^{(X)} + \mathbf{B}_{s_1 s_2 s_3}^{(Z)}. \tag{56}$$

Combining (49)-(56), we can write down the following decomposition for $\hat{\mathbf{X}}$.

$$\begin{aligned}
\hat{\mathbf{X}} &= \mathbf{Y}_{[\Omega_1, \Omega_2, \Omega_3]} \times_1 \bar{R}_1 \times_2 \bar{R}_2 \times_3 \bar{R}_3 \\
&= \left(\sum_{s_1, s_2, s_3=1}^2 \mathbf{B}_{s_1 s_2 s_3} \right) \times_1 (A_{11} J_{11}^{-1} + A_{12} J_{12}^{-1}) \times_2 (A_{21} J_{21}^{-1} + A_{22} J_{22}^{-1}) \times_3 (A_{31} J_{31}^{-1} + A_{32} J_{32}^{-1}) \\
&= \sum_{s_1, s_2, s_3=1}^2 \mathbf{B}_{s_1 s_2 s_3} \times_1 A_{1s_1} (J_{1s_1})^{-1} \times_2 A_{2s_2} (J_{2s_2})^{-1} \times_3 A_{3s_3} (J_{3s_3})^{-1}.
\end{aligned} \tag{57}$$

This form is very helpful in our analysis later.

4. In this step, we derive a few formulas for the terms in (57). To be specific, we shall prove the following results.

- Lower bound for singular value of the joint major part: for $t = 1, 2, 3$,

$$\sigma_{\min} \left(J_{t1}^{(X)} \right) \geq (1 - \tau_1^2)(1 - \tau^4 / (1 - 2\tau)^2) \sigma_{\min}(X_{\Omega_t \times \Xi_t}), \quad \tau_1 = \frac{\tau^2}{(1 - \tau^4 / (1 - 2\tau)^2 - \tau)^2 - \tau^2}. \quad (58)$$

In fact, according to definitions, $\hat{M}_t^\top X_{\Omega_t \times \Xi_t} \hat{N}_t = (J_{\hat{r}_t}^{(X)})_{[1:r_t, 1:r_t]}$, i.e., $\hat{M}_t^\top X_{\Omega_t \times \Xi_t} \hat{N}_t$ is a sub-matrix of $J_{\hat{r}_t}^{(X)}$, we have

$$\sigma_{r_t}(J_{\hat{r}_t}^{(X)}) \geq \sigma_{r_t} \left(\hat{M}^\top X_{\Omega_t \times \Xi_t} \hat{N} \right) \stackrel{(37)}{=} (1 - \tau^4 / (1 - 2\tau)^2) \sigma_{\min}(X_{\Omega_t \times \Xi_t}).$$

Let

$$\bar{K}_t \in \mathbb{O}_{\hat{r}_t, r_t}, \bar{L}_t \in \mathbb{O}_{\hat{r}_t, r_t} \text{ be the left and right singular vectors for rank-}r_t \text{ matrix } J_{\hat{r}_t}^{(X)}. \quad (59)$$

We summarize some facts here:

- $J_{\hat{r}_t} = J_{\hat{r}_t}^{(X)} + J_{\hat{r}_t}^{(Z)}$;
- \bar{K}_t, \bar{L}_t are the left and right singular vectors of rank- r_t matrix $J_{\hat{r}_t}^{(X)}$;
- K_{t1}, L_{t1} are the first r_t left and right singular vectors of $J_{\hat{r}_t}$.
- $\sigma_{r_t+1}(J_{\hat{r}_t}) \stackrel{\text{Weyl (1912)}}{\leq} \sigma_{r_t+1}(J_{\hat{r}_t}^{(X)}) + \|J_{\hat{r}_t}^{(Z)}\| \leq \tau \sigma_{\min}(X_{\Omega_t \times \Xi_t})$.
- $\sigma_{r_t}(J_{\hat{r}_t} \bar{L}_t) \stackrel{\text{Weyl (1912)}}{\geq} \sigma_{r_t}(J_{\hat{r}_t}^{(X)} \bar{L}_t) - \|J_{\hat{r}_t}^{(Z)}\| = \sigma_{r_t}(J_{\hat{r}_t}^{(X)}) - \|J_{\hat{r}_t}^{(Z)}\|$
 $\geq (1 - \tau^4 / (1 - 2\tau)^2 - \tau) \sigma_{\min}(X_{\Omega_t \times \Xi_t})$.

Then by the unilateral perturbation bound result (Proposition 1 and Lemma 1 in Cai and Zhang (2016)) and the facts above,

$$\begin{aligned} \|\sin \Theta(\bar{L}_t, L_{t1})\| &\leq \frac{\sigma_{r_t+1}(J_{\hat{r}_t}) \cdot \|\mathbb{P}_{(J_{\hat{r}_t} \bar{L}_t)} J_{\hat{r}_t}^{(Z)}\|}{\sigma_{r_t}^2(J_{\hat{r}_t} \bar{L}_t) - \sigma_{r_t+1}^2(J_{\hat{r}_t})} \stackrel{(60)}{\leq} \frac{\tau^2}{(1 - \tau^4 / (1 - 2\tau)^2 - \tau)^2 - \tau^2} := \tau_1. \\ \sigma_{\min}(L_{t1}^\top \bar{L}_t) &\geq \sqrt{1 - \tau_1^2}. \end{aligned}$$

Similarly, $\sigma_{\min}(K_{t1}^\top \bar{K}_t) \geq \sqrt{1 - \tau_1^2}$. Therefore,

$$\begin{aligned} \sigma_{\min} \left(J_{t1}^{(X)} \right) &= \sigma_{\min} \left(K_{t1}^\top J_{\hat{r}_t}^{(X)} L_{t1} \right) \stackrel{(59)}{=} \sigma_{\min} \left(K_{t1}^\top \mathbb{P}_{\bar{K}_t} J_{\hat{r}_t}^{(X)} \mathbb{P}_{\bar{L}_t} L_{t1} \right) = \sigma_{\min} \left(K_{t1}^\top \bar{K}_t \bar{K}_t^\top J_{\hat{r}_t}^{(X)} \bar{L}_t \bar{L}_t^\top L_{t1} \right) \\ &\geq \sigma_{\min}(K_{t1}^\top \bar{K}_t) \sigma_{\min} \left(\bar{K}_t^\top J_{\hat{r}_t}^{(X)} \bar{L}_t \right) \sigma_{\min}(L_{t1}^\top \bar{L}_t) \geq (1 - \tau_1^2) \sigma_{r_t}(J_{\hat{r}_t}^{(X)}) \\ &\geq (1 - \tau_1^2)(1 - \tau^4 / (1 - 2\tau)^2) \sigma_{\min}(X_{\Omega_t \times \Xi_t}). \end{aligned}$$

which has finished the proof for (58).

- Upper bound for all terms related to perturbation “Z:” for example,

$$\|J_{t1}^{(Z)}\| \leq \|Z_{\Omega_t \times \Xi_t}\| \leq \tau \sigma_{\min}(X_{\Omega_t \times \Xi_t}), \quad (60)$$

$$\|A_{t1}^{(Z)}\| \leq \|Z_{\Xi_t}\| \leq \tau \sigma_{\min}(X_{\Xi_t}).$$

$$\left\| \mathbf{B}_{s_1 s_2 s_3}^{(Z)} \right\|_{\text{HS}} \leq \|\mathbf{Z}_{[\Omega_1, \Omega_2, \Omega_3]}\|_{\text{HS}}, \quad \left\| \mathbf{B}_{s_1 s_2 s_3}^{(Z)} \right\|_{\text{op}} \leq \|\mathbf{Z}_{[\Omega_1, \Omega_2, \Omega_3]}\|_{\text{op}}. \quad (61)$$

Since all these terms related to perturbation “(Z)” are essentially projections of Z_{Ξ_t} , $Z_{\Omega_t \times \Xi_t}$, $Z_{t,\Omega}$ or $\mathbf{Z}_{[\Omega_1, \Omega_2, \Omega_3]}$, they can be derived easily.

- Upper bounds in spectral norm for “arm · joint⁻¹” and “joint⁻¹ · body”:

$$\left\| A_{t1}^{(X)} (J_{t1}^{(X)})^{-1} \right\| \leq \bar{\lambda}_t; \quad (62)$$

$$\text{if } (s_1, s_2, s_3) \in \{1, 2\}^3, t \in \{1, 2, 3\}, \quad \left\| (J_{ts_t}^{(X)})^{-1} \mathcal{M}_t(\mathbf{B}_{s_1 s_2 s_3}^{(X)}) \right\| \leq \xi_t; \quad (63)$$

$$\left\| A_{t1} (J_{t1})^{-1} \right\| \leq \bar{\lambda}_t + \frac{2\bar{\lambda}_t \tau}{(1 - \tau_1^2)(1 - \tau^4/(1 - 2\tau)^2) - \tau}; \quad (64)$$

$$\left\| A_{t2} (J_{t2})^{-1} \right\| \leq \lambda_t + \bar{\lambda}_t + \frac{2\bar{\lambda}_t \tau}{(1 - \tau_1^2)(1 - \tau^4/(1 - 2\tau)^2) - \tau}. \quad (65)$$

Recall (40) that $X_{\Xi_t} = U_t Q$, $X_{\Omega_t \times \Xi_t} = U_{t,\Omega} Q$, the definition for $A_{t1}^{(X)}$, $J_{t1}^{(X)}$ and the fact that $\sigma_{\min}(J_{t1}^{(X)}) > 0$, we have

$$\begin{aligned} \left\| A_{t1}^{(X)} (J_{t1}^{(X)})^{-1} \right\| &= \left\| \left(X_{\Xi_t} V_{t,[1:\hat{r}_t]}^{(A)} L_{t1} \right) \left(K_{t1}^\top U_{t,[1:\hat{r}_t]}^{(B)\top} X_{\Omega_t \times \Xi_t} V_{t,[1:\hat{r}_t]}^{(A)\top} L_{t1} \right)^{-1} \right\| \\ &= \left\| U_t Q V_{t,[1:\hat{r}_t]}^{(A)} L_{t1} \left(K_{t1}^\top U_{t,[1:\hat{r}_t]}^{(B)\top} U_{t,\Omega} Q V_{t,[1:\hat{r}_t]}^{(A)\top} L_{t1} \right)^{-1} \right\| \\ &= \left\| U_t Q V_{t,[1:\hat{r}_t]}^{(A)} L_{t1} \left(Q V_{t,[1:\hat{r}_t]}^{(A)\top} L_{t1} \right)^{-1} \left(K_{t1}^\top U_{t,[1:\hat{r}_t]}^{(B)\top} U_{t,\Omega} \right)^{-1} \right\| \\ &= \frac{1}{\sigma_{\min} \left(K_t^\top U_{t,[1:\hat{r}_t]}^{(B)\top} U_{t,\Omega} \right)} \leq \frac{1}{\sigma_{\min}(U_{t,\Omega})} = \bar{\lambda}_t, \end{aligned}$$

which has proved (62). The proof for (63) is similar. Since $X_{\Omega_t \times \Xi_t}$ is a collection of columns of $X_{t,\Omega}$ and $\text{rank}(X_{\Omega_t \times \Xi_t}) = \text{rank}(X_{t,\Omega}) = r_t$, these two matrices share the same column subspace. In this case,

$$X_{\Omega_t \times \Xi_t} \left(X_{\Omega_t \times \Xi_t}^\dagger X_{t,\Omega} \right) = \mathbb{P}_{X_{\Omega_t \times \Xi_t}} X_{t,\Omega} = X_{t,\Omega}.$$

Given the assumption (22) that $\|X_{\Omega_t \times \Xi_t}^\top X_{t,\Omega}\| \leq \xi_t$, the rest of the proof for (63) essentially follows from the proof for (62).

The proof for (64) is relatively more complicated. Note that

$$\begin{aligned} \|J_{t1}^{(Z)}\| &\leq \|Z_{\Omega_t \times \Xi_t}\| \leq \tau \sigma_{\min}(X_{\Omega_t \times \Xi_t}), \\ \|A_{t1}^{(Z)}\| &\leq \|Z_{\Xi_t}\| \leq \tau \sigma_{r_t}(X_{\Xi_t}) \leq \tau \sigma_{r_t}(Q) = \tau \sigma_{\min}(Q) \leq \frac{\tau \sigma_{\min}(U_{t,\Omega} Q)}{\sigma_{\min}(U_{t,\Omega})} \leq \tau \bar{\lambda}_t \sigma_{\min}(X_{\Omega_t \times \Xi_t}), \end{aligned} \quad (66)$$

we can calculate that

$$\begin{aligned} \|A_{t1} (J_{t1})^{-1}\| &= \left\| \left(A_{t1}^{(X)} + A_{t1}^{(Z)} \right) \left(J_{t1}^{(X)} + J_{t1}^{(Z)} \right)^{-1} \right\| \\ &\leq \|A_{t1}^{(X)} (J_{t1}^{(X)})^{-1}\| + \left\| A_{t1}^{(X)} \left(\left(J_{t1}^{(X)} + J_{t1}^{(Z)} \right)^{-1} - \left(J_{t1}^{(X)} \right)^{-1} \right) \right\| + \left\| A_{t1}^{(Z)} \left(J_{t1}^{(X)} + J_{t1}^{(Z)} \right)^{-1} \right\| \\ &\stackrel{\text{Lemma 5}}{=} \|A_{t1}^{(X)} (J_{t1}^{(X)})^{-1}\| + \left\| A_{t1}^{(X)} \left(J_{t1}^{(X)} \right)^{-1} J_{t1}^{(Z)} \left(J_{t1}^{(X)} + J_{t1}^{(Z)} \right)^{-1} \right\| + \|A_{t1}^{(Z)}\| \sigma_{\min}^{-1} \left(J_{t1}^{(X)} + J_{t1}^{(Z)} \right) \\ &\stackrel{(62)}{=} \bar{\lambda}_t + \bar{\lambda}_t \frac{\|J_{t1}^{(Z)}\|}{\sigma_{\min}(J_{t1}^{(X)}) - \|J_{t1}^{(Z)}\|} + \frac{\|A_{t1}^{(Z)}\|}{\sigma_{\min}(J_{t1}^{(X)}) - \|J_{t1}^{(Z)}\|} \\ &\stackrel{(66)(58)}{\leq} \bar{\lambda}_t + \frac{2\bar{\lambda}_t \tau}{(1 - \tau_1^2)(1 - \tau^4/(1 - 2\tau)^2) - \tau}. \end{aligned}$$

This has finished the proof for (64).

Next, we move on to (65). Recall the definitions of $A_{\hat{r}_t}$ and $J_{\hat{r}_t}$, and the fact that $K_{t1}, K_{t2}; L_{t1}, L_{t2}$ are orthogonal, we have $K_{t1}^\top K_{t1} = L_{t1}^\top L_{t1} = I$, $K_{t2}^\top K_{t2} = L_{t2}^\top L_{t2} = I$, $K_{t1}^\top K_{t2} = L_{t1}^\top L_{t2} = 0$. Then,

$$\begin{aligned} A_{\hat{r}_t} J_{\hat{r}_t}^{-1} &= \left(A_{\hat{r}_t} L_{t1} L_{t1}^\top + A_{\hat{r}_t} L_{t2} L_{t2}^\top \right) \left(K_{t1} K_{t1}^\top J_{\hat{r}_t} L_{t1} L_{t1}^\top + K_{t1} K_{t1}^\top J_{\hat{r}_t} L_{t2} L_{t2}^\top \right)^{-1} \\ &= \left(A_{t1} L_{t1}^\top + A_{t2} L_{t2}^\top \right) \left(K_{t1} J_{t1} L_{t1}^\top + K_{t2} J_{t2} L_{t2}^\top \right)^{-1} = \left(A_{t1} L_{t1}^\top + A_{t2} L_{t2}^\top \right) \left(L_{t1} J_{t1}^{-1} K_{t1}^\top + L_{t2} J_{t2}^{-1} K_{t2}^\top \right) \\ &= A_{t1} J_{t1}^{-1} K_{t1}^\top + A_{t2} J_{t2}^{-1} K_{t2}^\top. \end{aligned}$$

On the other hand, $\|A_{\hat{r}_t} J_{\hat{r}_t}^{-1}\| \leq \lambda_t$. Thus,

$$\begin{aligned} \|A_{t2} (J_{t2})^{-1}\| &\leq \|A_{\hat{r}_t} J_{\hat{r}_t}^{-1}\| + \|A_{t1} J_{t1}^{-1} K_{t1}^\top\| \\ &\leq \|A_{\hat{r}_t} J_{\hat{r}_t}^{-1}\| + \|A_{t1} J_{t1}^{-1}\| \leq \lambda_t + \bar{\lambda}_t + \frac{2\bar{\lambda}_t \tau}{(1 - \tau_1^2)(1 - \tau^4/(1 - 2\tau)^2) - \tau}, \end{aligned}$$

which has finished the proof for (65).

- Upper bounds in Frobenius and operator norm for “arm·(joint)⁻¹·body:” for the major part:

$$\left\| A_{t1} (J_{t1})^{-1} \mathcal{M}_t(B_{111}^{(X)}) - A_{t1}^{(X)} (J_{t1}^{(X)})^{-1} \mathcal{M}_t(B_{111}^{(X)}) \right\|_F \leq C \bar{\lambda}_t \xi_t \|Z_{\Omega_t \times \Xi_t}\|_F + C \xi_t \|Z_{\Xi_t}\|_F. \quad (67)$$

$$\left\| A_{t1} (J_{t1})^{-1} \mathcal{M}_t(B_{111}^{(X)}) - A_{t1}^{(X)} (J_{t1}^{(X)})^{-1} \mathcal{M}_t(B_{111}^{(X)}) \right\| \leq C \bar{\lambda}_t \xi_t \|Z_{\Omega_t \times \Xi_t}\| + C \xi_t \|Z_{\Xi_t}\|. \quad (68)$$

Actually, we can show that

$$\begin{aligned} & \left\| A_{t1} (J_{t1})^{-1} \mathcal{M}_t(B_{111}^{(X)}) - A_{t1}^{(X)} (J_{t1}^{(X)})^{-1} \mathcal{M}_t(B_{111}^{(X)}) \right\|_F \\ &= \left\| (A_{t1}^{(X)} + A_{t1}^{(Z)}) (J_{t1}^{(X)} + J_{t1}^{(Z)})^{-1} \mathcal{M}_t(B_{111}^{(X)}) - A_{t1}^{(X)} (J_{t1}^{(X)})^{-1} \mathcal{M}_t(B_{111}^{(X)}) \right\|_F \\ &\leq \left\| A_{t1}^{(X)} \left((J_{t1}^{(X)} + J_{t1}^{(Z)})^{-1} - (J_{t1}^{(X)})^{-1} \right) \mathcal{M}_t(B_{111}^{(X)}) \right\|_F + \left\| A_{t1}^{(Z)} (J_{t1}^{(X)} + J_{t1}^{(Z)})^{-1} \mathcal{M}_t(B_{111}^{(X)}) \right\|_F \\ &\stackrel{\text{Lemma 5}}{\leq} \left\| A_{t1}^{(X)} (J_{t1}^{(X)})^{-1} \left(J_{t1}^{(Z)} - J_{t1}^{(Z)} (J_{t1}^{(X)} + J_{t1}^{(Z)})^{-1} J_{t1}^{(Z)} \right) (J_{t1}^{(X)})^{-1} \mathcal{M}_t(B_{111}^{(X)}) \right\|_F \\ &\quad + \left\| A_{t1}^{(Z)} \left(- (J_{t1}^{(X)} + J_{t1}^{(Z)})^{-1} J_{t1}^{(Z)} + I \right) (J_{t1}^{(X)})^{-1} \mathcal{M}_t(B_{111}^{(X)}) \right\|_F \\ &\stackrel{(62)(63)}{\leq} C \bar{\lambda}_t \xi_t \left\| J_{t1}^{(Z)} - J_{t1}^{(Z)} (J_{t1}^{(X)} + J_{t1}^{(Z)})^{-1} J_{t1}^{(Z)} \right\|_F + C \xi_t \|A_{t1}^{(Z)}\|_F \cdot \left\| - (J_{t1}^{(X)} + J_{t1}^{(Z)})^{-1} J_{t1}^{(Z)} + I \right\| \\ &\stackrel{(60)(58)}{\leq} C \bar{\lambda}_t \xi_t \|J_{t1}^{(Z)}\|_F + C \xi_t \|A_{t1}^{(Z)}\|_F \\ &\leq C \bar{\lambda}_t \xi_t \|Z_{\Omega_t \times \Xi_t}\|_F + C \xi_t \|Z_{\Xi_t}\|_F. \end{aligned}$$

which has proved (67). The proof for (68) essentially follows from the proof for (67) when we replace the Frobenius norms with the spectral norm.

- Upper bounds for minor “body” part:

if $(s_1, s_2, s_3) \in \{1, 2\}^3$ and $s_t = 2$, then

$$\begin{cases} \|\mathbf{B}_{s_1 s_2 s_3}\|_{\text{HS}} \leq 2 \xi_t \|Z_{\Omega_t \times \Xi_t}\|_F + \|\mathbf{Z}_{[\Omega_1, \Omega_2, \Omega_3]}\|_{\text{HS}}, \\ \|\mathbf{B}_{s_1 s_2 s_3}\|_{\text{op}} \leq 2 \xi_t \|Z_{\Omega_t \times \Xi_t}\| + \|\mathbf{Z}_{[\Omega_1, \Omega_2, \Omega_3]}\|_{\text{op}}. \end{cases} \quad (69)$$

Instead of considering the “body” part above directly, we detour and discuss the “joint” part first. It is noteworthy that J_{t2} is the $r_t + 1, \dots, \hat{r}_t$ -th principle components for $J_{\hat{r}_t} = J_{\hat{r}_t}^{(X)} + J_{\hat{r}_t}^{(Z)}$. As $\text{rank}(J_{\hat{r}_t}^{(X)}) = r_t$, by Lemma 1 in Cai et al. (2016) (which provides inequalities of

singular values in the low-rank perturbed matrix),

$$\begin{aligned}
& \sigma_i(J_{t2}) = \sigma_{r_t+i}(J_{\hat{r}_t}) \leq \sigma_i(J_{\hat{r}_t}^{(Z)}), \quad \forall 1 \leq i \leq \hat{r}_t - r_t \\
\Rightarrow & \|J_{t2}\|_F = \sqrt{\sum_{i=1}^{\hat{r}_t-r_t} \sigma_i^2(J_{t2})} \leq \sqrt{\sum_{i=1}^{\hat{r}_t-r_t} \sigma_i^2(J_{\hat{r}_t}^{(Z)})} = \|J_{\hat{r}_t}^{(Z)}\|_F \leq \|Z_{\Omega_t \times \Xi_t}\|_F, \\
\Rightarrow & \|J_{t2}^{(X)}\|_F \leq \|J_{t2}\|_F + \|J_{t2}^{(Z)}\|_F \leq 2\|Z_{\Omega_t \times \Xi_t}\|_F, \\
\stackrel{(63)}{\Rightarrow} & \left\| \mathcal{M}_t(\mathbf{B}_{s_1 s_2 s_3}^{(X)}) \right\|_F \leq \left\| J_{t2}^{(X)} \right\|_F \cdot \left\| \left(J_{t2}^{(X)} \right)^{-1} \mathcal{M}_t(\mathbf{B}_{s_1 s_2 s_3}^{(X)}) \right\| \leq 2\xi_t \|Z_{\Omega_t \times \Xi_t}\|_F \\
\Rightarrow & \|\mathbf{B}_{s_1 s_2 s_3}\|_{\text{HS}} \leq \left\| \mathbf{B}_{s_1 s_2 s_3}^{(X)} \right\|_{\text{HS}} + \left\| \mathbf{B}_{s_1 s_2 s_3}^{(Z)} \right\|_{\text{HS}} \leq \|\mathcal{M}_t(\mathbf{B}_{s_1 s_2 s_3})\|_F + \|\mathbf{Z}_{[\Omega_1, \Omega_2, \Omega_3]}\|_{\text{HS}} \\
& \leq 2\xi_t \|Z_{\Omega_t \times \Xi_t}\|_F + \|\mathbf{Z}_{[\Omega_1, \Omega_2, \Omega_3]}\|_{\text{HS}}.
\end{aligned}$$

We can similarly derive that $\|\mathbf{B}_{s_1 s_2 s_3}\|_{\text{op}} \leq 2\xi_t \|Z_{\Omega_t \times \Xi_t}\| + \|\mathbf{Z}_{[\Omega_1, \Omega_2, \Omega_3]}\|_{\text{op}}$, which has proved (69).

- Equality for the original tensor \mathbf{X} :

$$\mathbf{X} = \mathbf{B}_{111}^{(X)} \times_1 A_{11}^{(X)} \left(J_{11}^{(X)} \right)^{-1} \times_2 A_{21}^{(X)} \left(J_{21}^{(X)} \right)^{-1} \times_3 A_{31}^{(X)} \left(J_{31}^{(X)} \right)^{-1}. \quad (70)$$

In fact, according to the definitions (50) - (56),

$$\begin{aligned}
& \mathbf{B}_{111}^{(X)} \times_1 A_{11}^{(X)} \times_2 A_{21}^{(X)} \times_3 A_{31}^{(X)} \\
= & \mathbf{X}_{[\Omega_1, \Omega_2, \Omega_3]} \\
& \times_1 X_{\Xi_1} \left(V_{1,[:,1:\hat{r}_1]}^{(A)} L_{11} \right) \left(\left(U_{1,[:,1:\hat{r}_1]}^{(B)} K_{11} \right)^\top X_{\Omega_1 \times \Xi_1} \left(V_{1,[:,1:\hat{r}_1]}^{(A)} L_{11} \right) \right)^{-1} \left(U_{1,[:,1:\hat{r}_1]}^{(B)} K_{11} \right)^\top \\
& \times_2 X_{\Xi_2} \left(V_{2,[:,1:\hat{r}_2]}^{(A)} L_{21} \right) \left(\left(U_{2,[:,1:\hat{r}_2]}^{(B)} K_{21} \right)^\top X_{\Omega_2 \times \Xi_2} \left(V_{2,[:,1:\hat{r}_2]}^{(A)} L_{21} \right) \right)^{-1} \left(U_{2,[:,1:\hat{r}_2]}^{(B)} K_{21} \right)^\top \\
& \times_3 X_{\Xi_3} \left(V_{3,[:,1:\hat{r}_3]}^{(A)} L_{31} \right) \left(\left(U_{3,[:,1:\hat{r}_3]}^{(B)} K_{31} \right)^\top X_{\Omega_3 \times \Xi_3} \left(V_{3,[:,1:\hat{r}_3]}^{(A)} L_{31} \right) \right)^{-1} \left(U_{3,[:,1:\hat{r}_3]}^{(B)} K_{31} \right)^\top.
\end{aligned}$$

Based on (58), $J_{t1}^{(X)} = K_{t1}^\top (U_{1,[:,1:\hat{r}_t]}^{(B)})^\top X_{\Omega_t \times \Xi_t} V_{t,[:,1:\hat{r}_t]}^{(A)} L_{t1}$ is non-singular, then by Theorem 1, we can show the term above equals \mathbf{X} , which has proved (70).

5. Now we are ready to analyze the estimation error of $\hat{\mathbf{X}}$ based on all the preparations in the

previous steps. Based on the decompositions of $\hat{\mathbf{X}}$ (57) and \mathbf{X} (70), one has

$$\begin{aligned}
& \left\| \hat{\mathbf{X}} - \mathbf{X} \right\|_{\text{HS}} \\
& \leq \left\| \mathbf{B}_{111} \times_1 A_{11} J_{11}^{-1} \times_2 A_{21} J_{21}^{-1} \times_3 A_{31} J_{31}^{-1} \right. \\
& \quad \left. - \mathbf{B}_{111}^{(X)} \times_1 A_{11}^{(X)} \left(J_{11}^{(X)} \right)^{-1} \times_2 A_{21}^{(X)} \left(J_{21}^{(X)} \right)^{-1} \times_3 A_{31}^{(X)} \left(J_{31}^{(X)} \right)^{-1} \right\|_{\text{HS}} \\
& \quad + \sum_{\substack{s_1, s_2, s_3=1 \\ (s_1, s_2, s_3) \neq (1, 1, 1)}}^2 \left\| \mathbf{B}_{s_1 s_2 s_3} \times_1 A_{1s_1} J_{1s_1}^{-1} \times_2 A_{2s_2} J_{2s_2}^{-1} \times_3 A_{3s_3} J_{3s_3}^{-1} \right\|_{\text{HS}} \\
& \leq \left\| \left(\mathbf{B}_{111} - \mathbf{B}_{111}^{(X)} \right) \times_1 A_{11} J_{11}^{-1} \times_2 A_{21} J_{21}^{-1} \times_3 A_{31} J_{31}^{-1} \right\|_{\text{HS}} \\
& \quad + \left\| \mathbf{B}_{111}^{(X)} \times_1 A_{11} J_{11}^{-1} \times_2 A_{21} J_{21}^{-1} \times_3 \left(A_{31} J_{31}^{-1} - A_{31}^{(X)} (J_{31}^{(X)})^{-1} \right) \right\|_{\text{HS}} \\
& \quad + \left\| \mathbf{B}_{111}^{(X)} \times_1 A_{11} J_{11}^{-1} \times_2 \left(A_{21} J_{21}^{-1} - A_{21}^{(X)} (J_{21}^{(X)})^{-1} \right) \times_3 A_{31}^{(X)} J_{31}^{(X)-1} \right\|_{\text{HS}} \\
& \quad + \left\| \mathbf{B}_{111}^{(X)} \times_1 \left(A_{11} J_{11}^{-1} - A_{11}^{(X)} (J_{11}^{(X)})^{-1} \right) \times_2 A_{21}^{(X)} J_{21}^{(X)-1} \times_3 A_{31}^{(X)} J_{31}^{(X)-1} \right\|_{\text{HS}} \\
& \quad + \sum_{\substack{s_1, s_2, s_3=1 \\ (s_1, s_2, s_3) \neq (1, 1, 1)}}^2 \left\| \mathbf{B}_{s_1 s_2 s_3} \times_1 A_{1s_1} J_{1s_1}^{-1} \times_2 A_{2s_2} J_{2s_2}^{-1} \times_3 A_{3s_3} J_{3s_3}^{-1} \right\|_{\text{HS}}.
\end{aligned} \tag{71}$$

For each term separately above, we have

$$\begin{aligned}
& \left\| \left(\mathbf{B}_{111} - \mathbf{B}_{111}^{(X)} \right) \times_1 A_{11} J_{11}^{-1} \times_2 A_{21} J_{21}^{-1} \times_3 A_{31} J_{31}^{-1} \right\|_{\text{HS}} \\
& \leq \|A_{11} J_{11}^{-1}\| \cdot \|A_{21} J_{21}^{-1}\| \cdot \|A_{31} J_{31}^{-1}\| \left\| \mathbf{B}_{111}^{(Z)} \right\|_{\text{HS}} \stackrel{(61)(62)}{\leq} C \lambda_1 \lambda_2 \lambda_3 \|\mathbf{Z}_{[\Omega_1, \Omega_2, \Omega_3]}\|_{\text{HS}}. \\
& \quad \left\| \mathbf{B}_{111}^{(X)} \times_1 A_{11} J_{11}^{-1} \times_2 A_{21} J_{21}^{-1} \times_3 \left(A_{31} J_{31}^{-1} - A_{31}^{(X)} (J_{31}^{(X)})^{-1} \right) \right\|_{\text{HS}} \\
& \leq \|A_{11} J_{11}^{-1}\| \cdot \|A_{21} J_{21}^{-1}\| \cdot \left\| \left(A_{31} J_{31}^{-1} - A_{31}^{(X)} (J_{31}^{(X)})^{-1} \right) \mathcal{M}_3(\mathbf{B}_{111}^{(X)}) \right\|_F \\
& \stackrel{(67)(62)}{\leq} C \lambda_1 \lambda_2 \lambda_3 \xi_3 \|Z_{\Omega_3 \times \Xi_3}\|_F + C \lambda_1 \lambda_2 \xi_3 \|Z_{\Xi_3}\|_F, \\
& \quad \left\| \mathbf{B}_{111}^{(X)} \times_1 A_{11} J_{11}^{-1} \times_2 \left(A_{21} J_{21}^{-1} - A_{21}^{(X)} (J_{21}^{(X)})^{-1} \right) \times_3 A_{31}^{(X)} J_{31}^{(X)-1} \right\|_{\text{HS}} \\
& \leq \|A_{11} J_{11}^{-1}\| \cdot \left\| A_{31}^{(X)} (J_{31}^{(X)})^{-1} \right\| \cdot \left\| \left(A_{21} J_{21}^{-1} - A_{21}^{(X)} (J_{21}^{(X)})^{-1} \right) \mathcal{M}_2(\mathbf{B}_{111}^{(X)}) \right\|_F \\
& \stackrel{(64)(67)(62)}{\leq} C \lambda_1 \lambda_2 \lambda_3 \xi_2 \|Z_{\Omega_2 \times \Xi_2}\|_F + C \lambda_1 \lambda_3 \xi_2 \|Z_{\Xi_2}\|_F, \\
& \quad \left\| \mathbf{B}_{111}^{(X)} \times_1 \left(A_{11} J_{11}^{-1} - A_{11}^{(X)} (J_{11}^{(X)})^{-1} \right) \times_2 A_{21}^{(X)} J_{21}^{(X)-1} \times_3 A_{31}^{(X)} J_{31}^{(X)-1} \right\|_{\text{HS}} \\
& \leq \left\| A_{21}^{(X)} (J_{21}^{(X)})^{-1} \right\| \cdot \left\| A_{31}^{(X)} (J_{31}^{(X)})^{-1} \right\| \cdot \left\| \left(A_{11} J_{11}^{-1} - A_{11}^{(X)} (J_{11}^{(X)})^{-1} \right) \mathcal{M}_1(\mathbf{B}_{111}^{(X)}) \right\|_F \\
& \stackrel{(64)(67)(62)}{\leq} C \lambda_1 \lambda_2 \lambda_3 \xi_1 \|Z_{\Omega_1 \times \Xi_1}\|_F + C \lambda_2 \lambda_3 \xi_1 \|Z_{\Xi_1}\|_F.
\end{aligned}$$

Last but not least, for any $s_1, s_2, s_3 \in \{1, 2\}^3$ such that $(s_1, s_2, s_3) \neq (1, 1, 1)$, let us specify that $s_t = 2$ for some $1 \leq t \leq 3$. Then

$$\begin{aligned} & \left\| \mathbf{B}_{s_1 s_2 s_3} \times_1 A_{1s_1} J_{1s_1}^{-1} \times_2 A_{2s_2} J_{2s_2}^{-1} \times_3 A_{3s_3} J_{3s_3}^{-1} \right\|_{\text{HS}} \\ & \leq \left\| A_{1s_1} J_{1s_1}^{-1} \right\| \cdot \left\| A_{2s_2} J_{2s_2}^{-1} \right\| \cdot \left\| A_{3s_3} J_{3s_3}^{-1} \right\| \cdot \left\| \mathbf{B}_{s_1 s_2 s_3} \right\|_{\text{HS}} \\ & \stackrel{(62)(65)(69)}{\leq} C \lambda_1 \lambda_2 \lambda_3 \left(\xi_t \|Z_{\Omega_t \times \Xi_t}\|_F + \|\mathbf{Z}_{[\Omega_1, \Omega_2, \Omega_3]}\|_{\text{HS}} \right). \end{aligned}$$

Combing all terms above, we have proved the following equality,

$$\left\| \hat{\mathbf{X}} - \mathbf{X} \right\|_{\text{HS}} \leq C \lambda_1 \lambda_2 \lambda_3 \left\| \mathbf{Z}_{[\Omega_1, \Omega_2, \Omega_3]} \right\|_{\text{HS}} + C \lambda_1 \lambda_2 \lambda_3 \sum_{t=1}^3 \xi_t \|Z_{\Omega_t \times \Xi_t}\|_{\text{HS}} + C \sum_{t=1}^3 \lambda_1 \lambda_2 \lambda_3 \frac{\xi_t}{\lambda_t} \|Z_{\Xi_t}\|_{\text{HS}}.$$

By similar argument, we can show the upper bound for $\|\hat{\mathbf{X}} - \mathbf{X}\|_{\text{op}}$,

$$\left\| \hat{\mathbf{X}} - \mathbf{X} \right\|_{\text{op}} \leq C \lambda_1 \lambda_2 \lambda_3 \left\| \mathbf{Z}_{[\Omega_1, \Omega_2, \Omega_3]} \right\|_{\text{op}} + C \lambda_1 \lambda_2 \lambda_3 \sum_{t=1}^3 \xi_t \|Z_{\Omega_t \times \Xi_t}\| + C \sum_{t=1}^3 \lambda_1 \lambda_2 \lambda_3 \frac{\xi_t}{\lambda_t} \|Z_{\Xi_t}\|.$$

Therefore, we have finished the proof for Theorem 2.

□

References

- Agarwal, A., Negahban, S., and Wainwright, M. J. (2012). Noisy matrix decomposition via convex relaxation: Optimal rates in high dimensions. *The Annals of Statistics*, pages 1171–1197.
- Barak, B. and Moitra, A. (2016). Noisy tensor completion via the sum-of-squares hierarchy. In *29th Annual Conference on Learning Theory*, pages 417–445.
- Bhojanapalli, S. and Sanghavi, S. (2015). A new sampling technique for tensors. *arXiv preprint arXiv:1502.05023*.
- Cai, T., Cai, T. T., and Zhang, A. (2016). Structured matrix completion with applications to genomic data integration. *Journal of the American Statistical Association*, 111(514):621–633.
- Cai, T. T. and Zhang, A. (2015). Rop: Matrix recovery via rank-one projections. *The Annals of Statistics*, 43(1):102–138.

- Cai, T. T. and Zhang, A. (2016). Rate-optimal perturbation bounds for singular subspaces with applications to high-dimensional statistics. *arXiv preprint arXiv:1605.00353*.
- Cai, T. T. and Zhou, W.-X. (2016). Matrix completion via max-norm constrained optimization. *Electronic Journal of Statistics*, 10(1):1493–1525.
- Candès, E. J. and Tao, T. (2010). The power of convex relaxation: Near-optimal matrix completion. *IEEE Transactions on Information Theory*, 56(5):2053–2080.
- Cao, Y. and Xie, Y. (2016). Poisson matrix recovery and completion. *IEEE Transactions on Signal Processing*, 64(6):1609–1620.
- Cao, Y., Zhang, A., and Li, H. (2016). Count zeros replacement in compositional data via multinomial matrix completion. *preprint*.
- Gandy, S., Recht, B., and Yamada, I. (2011). Tensor completion and low-n-rank tensor recovery via convex optimization. *Inverse Problems*, 27(2):025010.
- Gross, D. and Nesme, V. (2010). Note on sampling without replacing from a finite collection of matrices. *arXiv preprint arXiv:1001.2738*.
- Guhaniyogi, R., Qamar, S., and Dunson, D. B. (2015). Bayesian tensor regression. *arXiv preprint arXiv:1509.06490*.
- Hillar, C. J. and Lim, L.-H. (2013). Most tensor problems are np-hard. *Journal of the ACM (JACM)*, 60(6):45.
- Jain, P. and Oh, S. (2014). Provable tensor factorization with missing data. In *Advances in Neural Information Processing Systems*, pages 1431–1439.
- Jiang, X., Raskutti, G., and Willett, R. (2015). Minimax optimal rates for poisson inverse problems with physical constraints. *IEEE Transactions on Information Theory*, 61(8):4458–4474.
- Karatzoglou, A., Amatriain, X., Baltrunas, L., and Oliver, N. (2010). Multiverse recommendation: n-dimensional tensor factorization for context-aware collaborative filtering. In *Proceedings of the fourth ACM conference on Recommender systems*, pages 79–86. ACM.

- Keshavan, R. H., Oh, S., and Montanari, A. (2009). Matrix completion from a few entries. In *2009 IEEE International Symposium on Information Theory*, pages 324–328. IEEE.
- Kolda, T. G. and Bader, B. W. (2009). Tensor decompositions and applications. *SIAM review*, 51(3):455–500.
- Koltchinskii, V., Lounici, K., and Tsybakov, A. B. (2011). Nuclear-norm penalization and optimal rates for noisy low-rank matrix completion. *The Annals of Statistics*, pages 2302–2329.
- Kressner, D., Steinlechner, M., and Vandereycken, B. (2014). Low-rank tensor completion by riemannian optimization. *BIT Numerical Mathematics*, 54(2):447–468.
- Krishnamurthy, A. and Singh, A. (2013). Low-rank matrix and tensor completion via adaptive sampling. In *Advances in Neural Information Processing Systems*, pages 836–844.
- Li, L., Chen, Z., Wang, G., Chu, J., and Gao, H. (2014). A tensor prism algorithm for multi-energy ct reconstruction and comparative studies. *Journal of X-ray science and technology*, 22(2):147–163.
- Li, L. and Zhang, X. (2016). Parsimonious tensor response regression. *Journal of the American Statistical Association*, (just-accepted).
- Li, N. and Li, B. (2010). Tensor completion for on-board compression of hyperspectral images. In *2010 IEEE International Conference on Image Processing*, pages 517–520. IEEE.
- Li, X., Zhou, H., and Li, L. (2013). Tucker tensor regression and neuroimaging analysis. *arXiv preprint arXiv:1304.5637*.
- Liu, J., Musialski, P., Wonka, P., and Ye, J. (2013). Tensor completion for estimating missing values in visual data. *IEEE Transactions on Pattern Analysis and Machine Intelligence*, 35(1):208–220.
- Mahoney, M. W., Maggioni, M., and Drineas, P. (2008). Tensor-cur decompositions for tensor-based data. *SIAM Journal on Matrix Analysis and Applications*, 30(3):957–987.
- Mu, C., Huang, B., Wright, J., and Goldfarb, D. (2014). Square deal: Lower bounds and improved relaxations for tensor recovery. In *ICML*, pages 73–81.

- Negahban, S. and Wainwright, M. J. (2011). Estimation of (near) low-rank matrices with noise and high-dimensional scaling. *The Annals of Statistics*, pages 1069–1097.
- Nowak, R. D. and Kolaczyk, E. D. (2000). A statistical multiscale framework for poisson inverse problems. *IEEE Transactions on Information Theory*, 46(5):1811–1825.
- Rauhut, H., Schneider, R., and Stojanac, Z. (2016). Low rank tensor recovery via iterative hard thresholding. *arXiv preprint arXiv:1602.05217*.
- Recht, B. (2011). A simpler approach to matrix completion. *Journal of Machine Learning Research*, 12(Dec):3413–3430.
- Rendle, S. and Schmidt-Thieme, L. (2010). Pairwise interaction tensor factorization for personalized tag recommendation. In *Proceedings of the third ACM international conference on Web search and data mining*, pages 81–90. ACM.
- Rohde, A., Tsybakov, A. B., et al. (2011). Estimation of high-dimensional low-rank matrices. *The Annals of Statistics*, 39(2):887–930.
- Semerci, O., Hao, N., Kilmer, M. E., and Miller, E. L. (2014). Tensor-based formulation and nuclear norm regularization for multienergy computed tomography. *IEEE Transactions on Image Processing*, 23(4):1678–1693.
- Shah, P., Rao, N., and Tang, G. (2015). Optimal low-rank tensor recovery from separable measurements: Four contractions suffice. *arXiv preprint arXiv:1505.04085*.
- Srebro, N. and Shraibman, A. (2005). Rank, trace-norm and max-norm. In *International Conference on Computational Learning Theory*, pages 545–560. Springer.
- Sun, W. W. and Li, L. (2016). Sparse low-rank tensor response regression. *arXiv preprint arXiv:1609.04523*.
- Sun, W. W., Lu, J., Liu, H., and Cheng, G. (2015). Provable sparse tensor decomposition. *Journal of Royal Statistical Association*.
- Tucker, L. R. (1966). Some mathematical notes on three-mode factor analysis. *Psychometrika*, 31(3):279–311.

- Vershynin, R. (2010). Introduction to the non-asymptotic analysis of random matrices. *arXiv preprint arXiv:1011.3027*.
- Weyl, H. (1912). Das asymptotische verteilungsgesetz der eigenwerte linearer partieller differentialgleichungen (mit einer anwendung auf die theorie der hohlraumstrahlung). *Mathematische Annalen*, 71(4):441–479.
- Yuan, M. and Zhang, C.-H. (2014). On tensor completion via nuclear norm minimization. *Foundations of Computational Mathematics*, pages 1–38.
- Yuan, M. and Zhang, C.-H. (2016). Incoherent tensor norms and their applications in higher order tensor completion. *arXiv preprint arXiv:1606.03504*.
- Zhang, A., Brown, L. D., and Cai, T. T. (2016). Semi-supervised inference: General theory and estimation of means. *arXiv preprint arXiv:1606.07268*.
- Zhou, H., Li, L., and Zhu, H. (2013). Tensor regression with applications in neuroimaging data analysis. *Journal of the American Statistical Association*, 108(502):540–552.